JACS
JOURNAL OF THE AMERICAN CHEMICAL SOCIETY
Article
pubs.acs.org/JACS
Open Access on 08/15/2015

Total Synthesis of Viridicatumtoxin B and Analogues Thereof: Strategy Evolution, Structural Revision, and Biological Evaluation

K. C. Nicolaou,*[,†,‡,#] Christopher R. H. Hale,[†,‡,⊥,#] Christian Nilewski,[†,‡,⊥,#] Heraklidia A. Ioannidou,[†,‡,#] Abdelatif ElMarrouni,[†,‡,#] Lizanne G. Nilewski,[†,‡,#] Kathryn Beabout,[§] Tim T. Wang,[§] and Yousif Shamoo[§,∥]

[†]Department of Chemistry, [§]Department of Biochemistry and Cell Biology, and [∥]Department of Ecology and Evolutionary Biology, Rice University, 6100 Main Street, Houston, Texas 77005, United States

[‡]Department of Chemistry, The Scripps Research Institute, 10550 North Torrey Pines Road, La Jolla, California 92037, United States

Supporting Information

ABSTRACT: The details of the total synthesis of viridicatumtoxin B (**1**) are described. Initial synthetic strategies toward this intriguing tetracycline antibiotic resulted in the development of key alkylation and Lewis acid-mediated spirocyclization reactions to form the hindered EF spirojunction, as well as Michael−Dieckmann reactions to set the A and C rings. The use of an aromatic A-ring substrate, however, was found to be unsuitable for the introduction of the requisite hydroxyl groups at carbons 4a and 12a. Applying these previous tactics, we developed stepwise approaches to oxidize carbons 12a and 4a based on enol- and enolate-based oxidations, respectively, the latter of which was accomplished after systematic investigations that revealed critical reactivity patterns. The herein described synthetic strategy resulted in the total synthesis of viridicatumtoxin B (**1**), which, in turn, formed the basis for the revision of its originally assigned structure. The developed chemistry facilitated the synthesis of a series of viridicatumtoxin analogues, which were evaluated against Gram-positive and Gram-negative bacterial strains, including drug-resistant pathogens, revealing the first structure−activity relationships within this structural type.

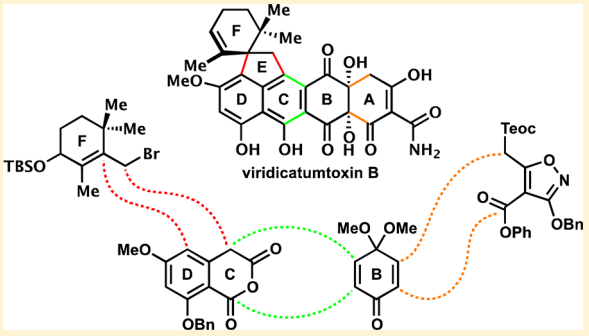

INTRODUCTION

Within the class of tetracycline antibiotics, viridicatumtoxin B (**1**),[1] viridicatumtoxin A (**2**),[2] and spirohexaline (**3**)[3] (Chart 1) are unique in that they include in their structures a geranyl-derived subunit in the form of a spirobicyclic system (ring system EF). In contrast to the majority of tetracyclines, these members of the group are also distinguished by their fungal, rather than bacterial, origins. The subject of this article is the pursuit of viridicatumtoxin B (**1**) by total synthesis, its full structural elucidation, and investigation of its antibacterial properties as well as those of selected synthetic analogues. The following brief historical overview places the present work and its aims in perspective within the field of tetracycline antibiotics.

Chart 1. Molecular Structures of Viridicatumtoxins 1−3

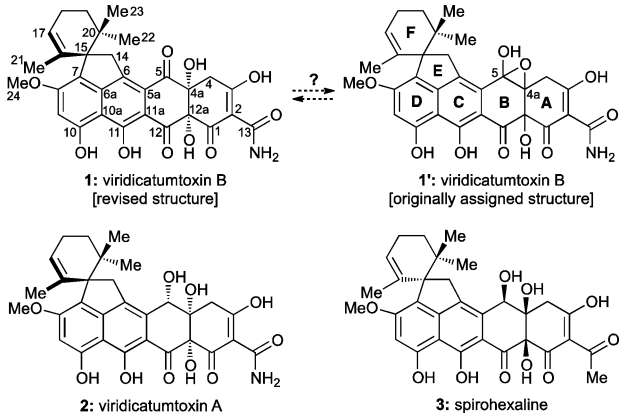

The discovery of chlortetracycline (**4**, Chart 2a), the first tetracycline antibiotic, by B. M. Duggar of the American Cyanamid Corporation in the late 1940s ushered in a new subclass of antibacterial agents at the dawn of the golden era of antibiotics.[4] The widespread success of tetracyclines in curing previously high-mortality-rate diseases bestowed on them the status of "wonder drug" shortly after their introduction into the clinic.[5] Since the discovery of chlortetracycline and other first-generation tetracyclines [e.g., oxytetracycline (**5**) and tetracycline (**6**), Chart 2a], second-generation tetracyclines, including minocycline (**7**) and doxycycline (**8**) (Chart 2a), emerged with improved properties. More recently, third-generation tetracyclines such as tigecycline (**9**)[6] and eravacycline (TP-434, **10**)[7] (Chart 2a) that overcome certain bacterial resistance mechanisms have been introduced.[8]

Received: June 27, 2014
Published: August 15, 2014

   dx.doi.org/10.1021/ja506472u | J. Am. Chem. Soc. 2014, 136, 12137−12160

Chart 2. Molecular Structures of (a) Bacterial Tetracyclines and Designed Analogues and (b) Fungal Tetracyclines

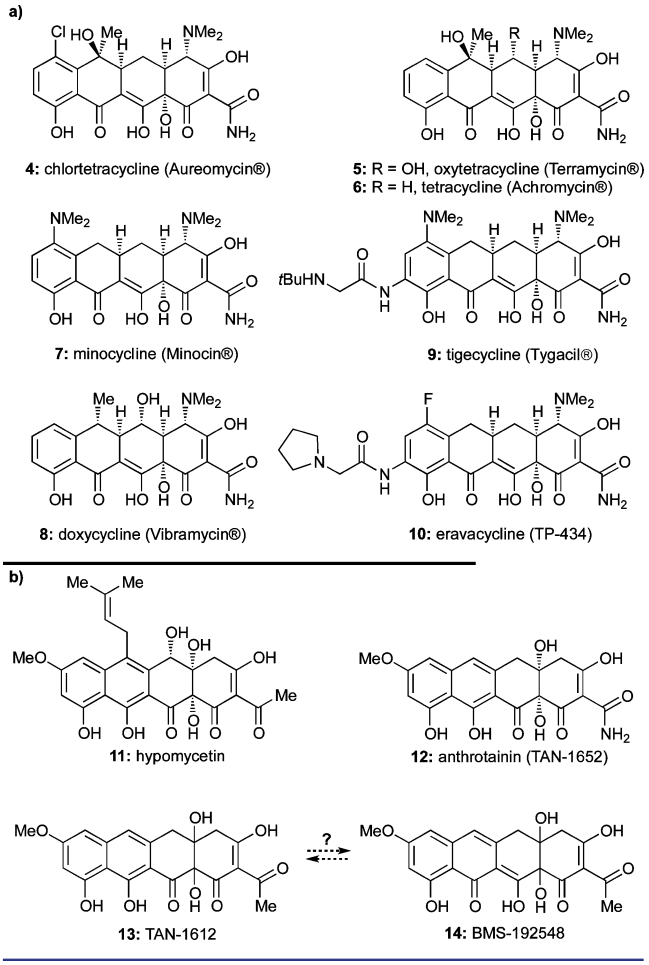

Scheme 1. Proposed Biosynthesis of the Terpene-Derived Spirocyclic Region of Viridicatumtoxin A (2)

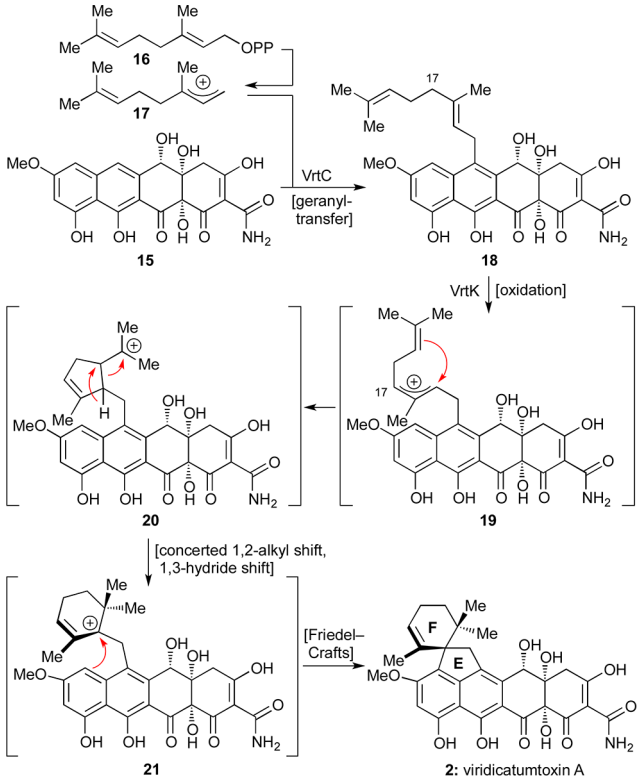

Most naturally occurring tetracyclines are produced by bacterial strains, although a few have been isolated from fungi. Thus, in addition to those shown in Chart 1 (**1**–**3**), hypomycetin (**11**),[9] anthrotainin (TAN-1652, **12**),[10] TAN-1612 (**13**),[11] and BMS-192548 (**14**)[12] (Chart 2b) are fungal metabolites.

Due to their complex structures and important biological activities, tetracyclines have been the subject of numerous synthetic campaigns since the 1950s. Noteworthy achievements in tetracycline synthesis include those recorded by Woodward/Pfizer,[13] Shemyakin,[14] Muxfeldt,[15] Barton,[16] Wasserman/Scott,[17] Stork,[18] Tatsuta,[19] and, more recently, Myers[20] and Evans.[21]

First isolated in 1973 from a *Penicillium* strain in South Africa, viridicatumtoxin A (**2**) yielded to X-ray crystallographic analysis in 1976.[2,22] The biosynthesis of this antibiotic was studied by the groups of Vleggaar[23] and, more recently, Tang and co-workers,[24] the latter of whom proposed a complete biosynthetic pathway. Specifically, as shown in Scheme 1, it was suggested that the EF-spirosystem is formed from polyketide **15** and a unit of geranyl pyrophosphate (**16**) as facilitated by VrtC, a polyketide prenyltransferase.[25] This reaction is followed by oxidative cyclization catalyzed by another Vrt enzyme (VrtK, a cytochrome P450-type enzyme)[26] to afford viridicatumtoxin A (**2**) through transient intermediates **19**–**21** (on the basis of computational studies), as shown in Scheme 1.

In 2008, Kim et al.[1] reported the isolation of viridicatumtoxin B in small quantities along with viridicatumtoxin A (**2**) from *Penicillium* sp. FR11 and, on the basis of NMR spectroscopic analysis, assigned the hydroxy-epoxide structure **1′** (Chart 1) to the former. These investigators observed potent activities for viridicatumtoxins A and B against Gram-positive bacteria, including methicillin-resistant *Staphylococcus aureus* (MRSA) (MIC = 0.25 and 0.5 μg/mL, respectively). Interestingly, a recent report suggested that the viridicatumtoxins exert their antibacterial properties through inhibition of UPP synthase, an important enzyme for bacterial peptidoglycan biosynthesis.[3,27] This stands in contrast to the mode of action of other tetracyclines (e.g., **4**–**10**, Chart 2a), which inhibit bacterial protein synthesis by binding to the 30S subunit of the ribosome.

In view of the scarcity of viridicatumtoxin B, its interesting but suspect structural assignment (i.e., **1′**, Chart 1), and its important biological activity, we initiated a program directed toward its total synthesis. Herein, we describe details of our investigations that led to important new knowledge and insights with regard to this intriguing bioactive molecule.[28]

RESULTS AND DISCUSSION

First-Generation Approach: Development of an Anthrone Alkylation and Lewis Acid-Mediated Spirocyclization. The intrigue surrounding the originally assigned structure of viridicatumtoxin B (**1′**) is derived from its uncommon epoxy-hemiacetal structural motif, its lipophilic spirocyclic domain, and its high oxygenation, particularly on ring B. Although the first and rather curious structural feature may have an explanation in this instance originating from the surrounding functionalities of the molecule, from the synthetic point of view, it was reasoned that it could be resolved by

dx.doi.org/10.1021/ja506472u | J. Am. Chem. Soc. 2014, 136, 12137–12160

targeting either structure **1′** or **1** (Chart 1) and allowing their potential thermodynamic equilibration to provide an answer. The spirocycle provided a synthetic challenge that we decided to face following the proposed biosynthesis, which inspired a Friedel–Crafts-type approach (see Scheme 1). The remaining major challenge of a synthesis of viridicatumtoxin B was initially relegated to a rather speculative singlet oxygen [4 + 2] cycloaddition to an appropriately substituted aromatic ring (B). Finally, the construction of the enol–amide structural motif characteristic of most tetracyclines was to be derived from an isoxazole ring through hydrogenolysis, a well-tested and reliable tactic introduced by Stork and Hagedorn.[18a]

These considerations led to our first retrosynthetic analysis of viridicatumtoxin B as depicted in Scheme 2. Thus, it was

Scheme 2. First-Generation Retrosynthetic Analysis through Endoperoxide 23

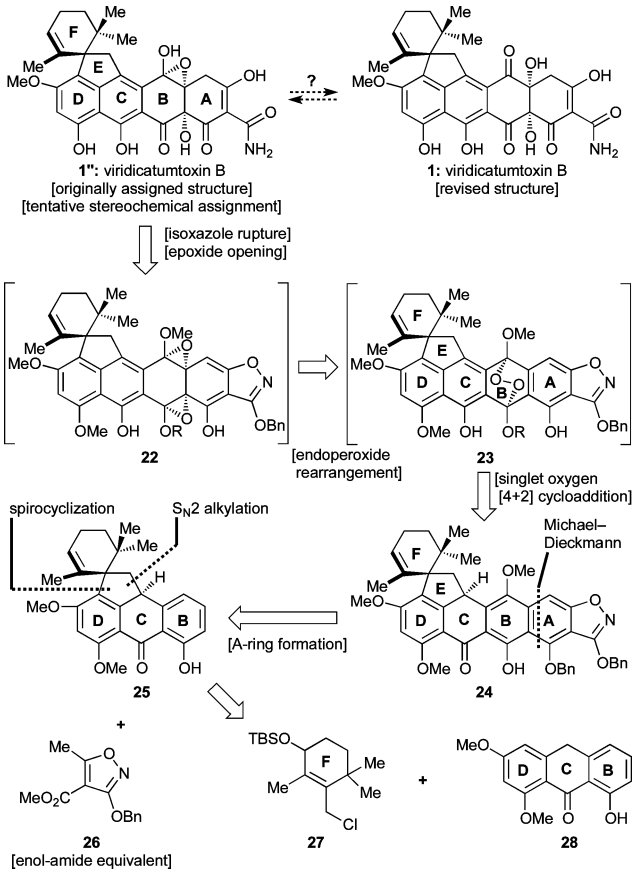

reasoned that **1″** or **1** could be derived from bis-epoxide structure **22** (R = selectively cleavable protecting group), which could be traced to endoperoxide **23** through a radical-based rearrangement and thence to aromatic system **24** via selective oxygen addition to the electron-rich B-ring. This scenario was inspired by a number of previous relevant studies, highlights of which are shown in Scheme 3.[29] Thus, endoperoxide **29** (generated from singlet oxygen and tetracene) was reported to undergo a thermally-induced rearrangement to bis-epoxide **31**, presumably via diradical **30**, and the latter was trapped with *N*-methylmaleimide (**32**) to afford adduct **33** (Scheme 3a).[29e] The regioselectivity of the latter reaction is of note in that it reflects different reactivities for the benzene and naphthalene systems. A similar type of fragmentation was induced within

Scheme 3. Precedent for Arene–Endoperoxide Rearrangements Based on (a) Thermal-, (b) Redox-, and (c) Photo-Induced O–O Bond Cleavage

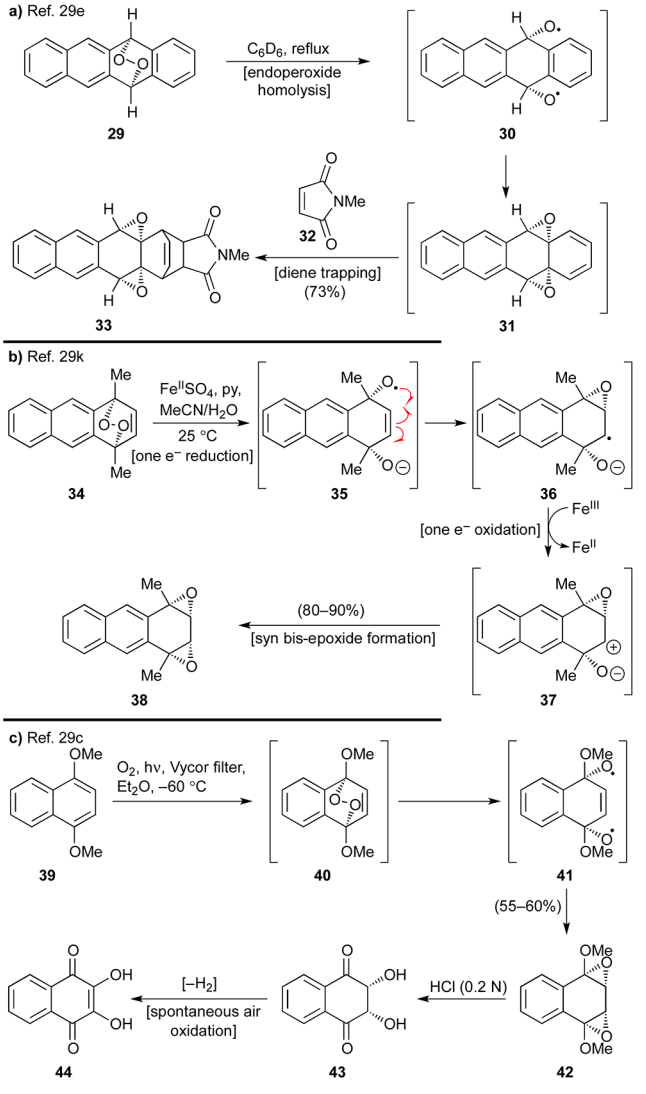

endoperoxide **34** by an iron(II) species, leading to bis-epoxide **38**, as shown in Scheme 3b.[29k] This rearrangement is presumed to proceed through the sequential one-electron transfers involving transient species **35**–**37**.[30,31] Photochemically-induced homolytic rupture of endoperoxides is also possible as demonstrated in Scheme 3c.[29c] Specifically, endoperoxide **40**, generated from naphthalene derivative **39**, formed bis-epoxide **42**, presumably via diradical **41**. Further elaboration of **42** led first to syn diol **43** and thence dihydroxy quinone **44**, demonstrating the accessibility and versatility of the endoperoxide moiety.[32]

The synthesis of allylic chloride fragment **27** began with geranic acid (**45**) and followed a modified sequence based on a literature process,[33] as shown in Scheme 4. Thus, acid-mediated cationic cyclization (H_3PO_4) of **45** followed by methylation (MeI, K_2CO_3) of the resulting acid produced methyl ester **46**. Epoxidation of the latter with *m*-CPBA furnished a mixture of epoxide isomers which was treated with NaOMe to give the desired allylic alcohol methyl ester **47** (70% for four steps). Protection of the hydroxyl group of **47** (TBSCl, imid.) and subsequent reduction (DIBAL-H) then led to allylic alcohol **48**

dx.doi.org/10.1021/ja506472u | J. Am. Chem. Soc. 2014, 136, 12137–12160

Scheme 4. Synthesis of Allylic Chloride 27[a]

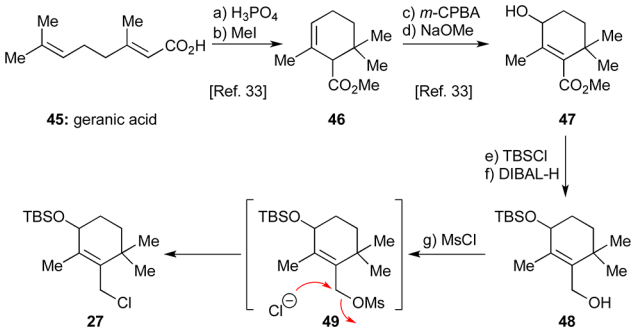

[a]Reagents and conditions: (a) H_3PO_4 (0.2 equiv), toluene, reflux, 90 min; (b) MeI (3.9 equiv), K_2CO_3 (2.0 equiv), acetone, 25 °C, 15 h; (c) *m*-CPBA (1.2 equiv), CH_2Cl_2, 0 → 25 °C, 3 h; (d) NaOMe (1.5 equiv), MeOH, reflux, 17 h, 70% for four steps; (e) TBSCl (1.6 equiv), imidazole (2.0 equiv), CH_2Cl_2, 25 °C, 12 h; (f) DIBAL-H (2.7 equiv), CH_2Cl_2, −78 → 0 °C, 70 min, 91% for two steps; (g) MsCl (1.2 equiv), Et_3N (1.5 equiv), DMAP (0.05 equiv), CH_2Cl_2, 25 °C, 14 h; then LiCl (1.0 equiv), 42 h, 48%. *m*-CPBA = *meta*-chloroperoxybenzoic acid, TBS = *tert*-butyldimethylsilyl, DIBAL-H = diisobutylaluminum hydride, Ms = methanesulfonyl, DMAP = 4-dimethylaminopyridine.

(91% for two steps). Attempted mesylation of **48** with MsCl/Et_3N led to partial formation of allylic chloride **27**, presumably via the initially formed mesylate **49**. It was then found that treatment of **48** with MsCl/Et_3N followed by addition of LiCl produced the allylic chloride **27** in satisfactory yield (48%).

With allylic chloride **27** readily available, we next turned our attention to the construction of anthrone **28** (Scheme 5). Bromo-benzyl juglone **51** was prepared in 66% overall yield following a two-step literature procedure starting from juglone (**50**).[34] Known Brassard diene **53** was prepared in one step starting from methyl 3-methoxybut-2-enoate (**52**) via formation of the corresponding enolate and subsequent trapping with TMSCl (99%).[35] With these building blocks in hand, their fusion through a Diels–Alder reaction was performed by mixing the dienophile **51** with 3 equiv of diene **53** at −30 °C and allowing the reaction mixture to reach ambient temperature. The TMS ether of the initially formed Diels–Alder adduct **54** was cleaved with silica gel, which caused collapse of the ketal and spontaneous elimination of HBr (see **55**, Scheme 5) followed by tautomerization, ultimately producing anthraquinone **56** in 90% overall yield. Similar types of cascade Diels–Alder/elimination sequences have been performed previously.[36] Methylation of the free phenolic group of **56** (MeI, K_2CO_3) followed by regioselective deoxygenation ($SnCl_2$, HCl/AcOH) and concomitant debenzylation then furnished anthrone **28** (86% yield for two steps).[37]

Previous reports have detailed the successful alkylation of the methylene position of anthrones with simple alkyl halides.[38] These studies also provided precedent for alkylation at the methylene position in preference to the free phenolic position(s), the latter being deactivated by hydrogen bonding with the adjacent carbonyl group. Nevertheless, the alkylation of an anthrone with a more complex electrophile was unprecedented and had not been utilized previously in the context of tetracycline synthesis. It was, therefore, pleasing to find that union of anthrone **28** with chloride **27** was successful when performed at 50 °C, employing Na_2CO_3 as the base in the presence of catalytic quantities of KI, providing the desired

Scheme 5. Synthesis of Spirocycle 25 and Conformational Rationale for Its Stereoselective Formation[a]

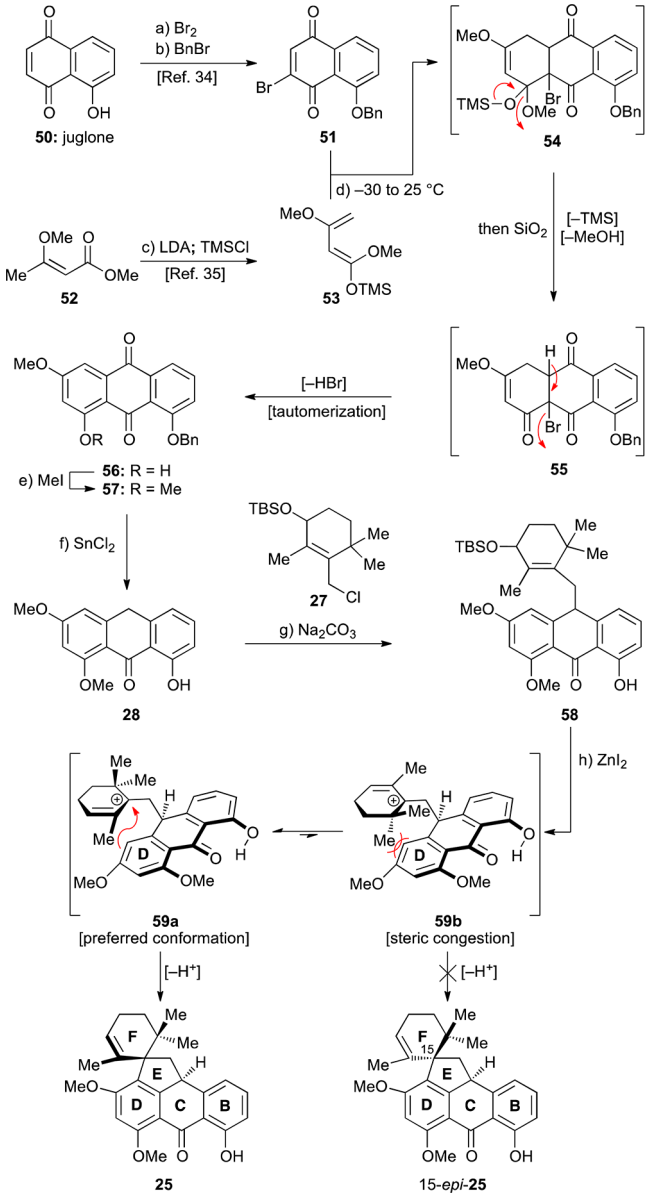

[a]Reagents and conditions: (a) Br_2 (1.03 equiv), AcOH, 25 °C, 30 min; then EtOH, reflux, 15 min; (b) BnBr (2.1 equiv), Ag_2O (2.1 equiv), CH_2Cl_2, 25 °C, 18 h, 66% for two steps; (c) LDA (1.05 equiv), THF, −78 °C, 1 h; then TMSCl (1.2 equiv), −78 → 25 °C, 100 min, 99%; (d) **51** (1.0 equiv), **53** (3.0 equiv), CH_2Cl_2, −30 → 25 °C, 70 min; then SiO_2 (excess), 1 h, 90%; (e) MeI (5.0 equiv), K_2CO_3 (5.0 equiv), DMF, 65 °C, 14 h; (f) $SnCl_2$ (7.0 equiv), AcOH:HCl 10:1, 50 °C, 86% for two steps; (g) **27** (1.0 equiv), KI (0.1 equiv), Na_2CO_3 (2.5 equiv), acetone, 50 °C, 18 h, 51%, ca. 1:1 dr; (h) ZnI_2 (0.78 equiv), CH_2Cl_2, reflux, 25 h, 34%. Bn = benzyl, THF = tetrahydrofuran, LDA = lithium diisopropylamide, TMS = trimethylsilyl.

product **58** in 51% yield (ca. 1:1 dr). It is worth noting that the success of this reaction depended on degassing the solution and conducting the reaction in the absence of light[39] to prevent oxidative radical dimerization of the anthrone substrate.[40]

Initial attempts to form the EF spirosystem were based on precedents that typically employed unprotected allylic alcohols[41] or allylic acetates[42] as the cationic precursors. However, most attempts to remove the TBS group of intermediate **58**

dx.doi.org/10.1021/ja506472u | J. Am. Chem. Soc. 2014, 136, 12137−12160

were complicated with side-products, including elimination or allylic substitution products (e.g., allylic methyl ether with HCl/MeOH). These observations led us to hypothesize that it might be possible to directly ionize the TBS ether of **58**, thereby eliminating the need for the deprotection step. After a brief screen of acidic conditions, it was found that ZnI_2 indeed promoted the desired transformation in 34% yield. As shown in Scheme 5, portionwise treatment of allylic TBS ether **58** in refluxing CH_2Cl_2 with ZnI_2 produced spirocyclic compound **25** as a single detectable diastereomer. This reaction presumably proceeds via ionization of the TBS ether to generate allylic cation **59a/b**. Then, intramolecular Friedel–Crafts-type reaction with the more electron-rich arene (ring D) followed by loss of a proton produces the observed product **25**. We did not isolate any product resulting from Friedel–Crafts reaction on the B-ring, although some elimination products were observed. While the yield of this transformation was, for the time, rather modest, it was sufficient to allow us to probe the following steps. The stereochemical configuration of **25** was assigned by comparison with subsequent intermediates whose structures were unambiguously deduced from X-ray crystallographic studies (see below). The observed diastereoselectivity of the spirocyclization (**58** → **25**) can be rationalized by invoking the transition state resulting from conformer **59a** as having the lowest energy barrier, as shown in Scheme 5. The transition state resulting from alternative conformer **59b**, required to afford the other (15-*epi*-**25**, undesired) diastereomer, suffers from unfavorable interactions between one of the methyl groups and the arene, as indicated in structure **59b**. These interactions are apparently not present in the transition state leading to the observed product (**59a** → **25**).

As shown in Scheme 6, we next needed to perform a phenolic oxidation to render the B-ring of the growing molecule electrophilic, and thereby susceptible, to nucleophilic attack from a negatively charged A-ring isoxazole (i.e., anion of **26**, see Scheme 2). The prototypical sequence of events for achieving this objective would involve PIDA [$PhI(OAc)_2$]- or PIFA [$PhI(TFA)_2$]-mediated oxidation of the phenolic moiety of **25** in MeOH to give intermediate **60**, which may undergo a second oxidation to yield the desired quinone monoketal **61**.[43] In reality, however, **25** proved intransigent to these projected transformations, leaving quinone monoketal **61** and its relatives, **60** and **64**, elusive under a variety of conditions tested. These included hypervalent iodine-, molecular oxygen-, and metal-based oxidative conditions (see Supporting Information for details). Instead, benzylic oxidation leading to quinomethide **62** was observed in several cases, as well as decomposition under different conditions. In a few cases, undesired products involving oxidation of the F-ring were also observed.

Eventually, it was found that spirocycle **25** could be tautomerized to its desmotropic form **63** under basic conditions (i.e., K_2CO_3, Scheme 6).[44] When the latter compound was treated with PIDA in CH_2Cl_2/H_2O the desired quinone **64** could be isolated in only 4% yield, along with substantial quantities of benzylic oxidation product **62** (13%) and recovered starting material (45%). A number of different oxidants (i.e., Fremy's salt, O_2/salcomine catalyst, PIFA) were examined in efforts to improve the efficiency of the transformation of **63** to quinone **64**, but unfortunately to no avail.

Unable to access quinone **64** in sufficient quantities, it was decided to focus our attention on an approach that would directly bring in the A-ring from an earlier stage, which would circumvent the problematic B-ring phenolic oxidation barriers we faced. Despite its failure to break through these barriers, however, the initial approach provided us with useful information and methods for the construction of the anthrone and allylic halide substrates and established the required spirocyclization reaction.

Scheme 6. Attempted Phenolic Oxidation of 25 and 63[a]

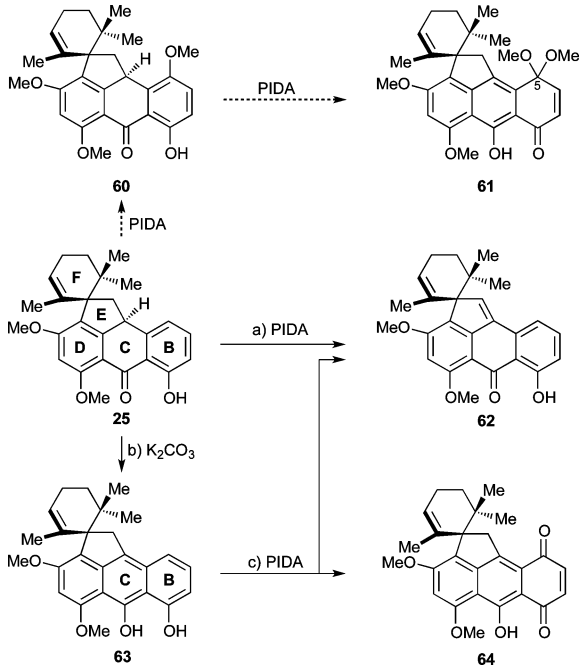

[a]Reagents and conditions: (a) $PhI(OAc)_2$ (3.0 equiv), MeOH, 25 °C, 43 h, 37% for **62** + 26% recovered **25**; (b) K_2CO_3 (2.4 equiv), MeOH, 25 °C, 10 min, 54%; (c) $PhI(OAc)_2$ (2.5 equiv), CH_2Cl_2:H_2O 7:1, 0 → 25 °C, 55 min, 4% for **64**, 13% for **62**, 45% recovered **63**. PIDA = phenyliodonium diacetate.

Second-Generation Approach: Attempts To Install the C4a and C12a Hydroxyl Groups via Dearomatization Pathways. The second-generation retrosynthesis of substrate **24**, required for our endoperoxide rearrangement approach (see Scheme 2), is shown in Scheme 7. Thus, to avoid the oxidation problems discussed above, the subtarget molecule **24** was dissected through the C-ring, which retrosynthetically defined three fragments: allylic chloride **27**, known homophthalic anhydride **66**,[45] and AB-enone **65**. The latter could be further disassembled into known quinone monoketal **67**[46] and Stork–Hagedorn isoxazole **26**.[18a]

The synthesis of requisite AB-enone **65** commenced from the known Stork–Hagedorn isoxazole **26**, which was prepared using a modification of the literature procedure (see Scheme 8). Thus, the process for the synthesis of **26** involved acylation of dimethyl malonate (**68**) ($MgCl_2$, Et_3N, AcCl, 96%),[47] methylation of the resulting enol (**69**) with Me_2SO_4 (54%), cyclization of **70** with H_2NOH to afford compound **71** (48%), and benzylation of the resulting hydroxy-isoxazole (BnBr, Ag_2O, 67%). The best conditions we found for the benzylation reaction were those employing Ag_2O which provided the *O*-Bn in preference to the *N*-Bn product in ratios of up to 11:1. Alternative conditions gave unacceptably low selectivity ratios (Cs_2CO_3/BnBr: *O*:*N* ca. 1.25:1; TfOH/BnTCA: *O*:*N* ca. 1:7.5) in agreement with Kornblum's rule for ambident nucleophiles.[48] A procedure using phenyldiazomethane as the electrophile as used by Stork and co-workers[18a] was considered

dx.doi.org/10.1021/ja506472u | J. Am. Chem. Soc. 2014, 136, 12137–12160

Scheme 7. Second-Generation Retrosynthetic Analysis of Viridicatumtoxin B (1 or its isomer 1″) through Endoperoxide Precursor 24

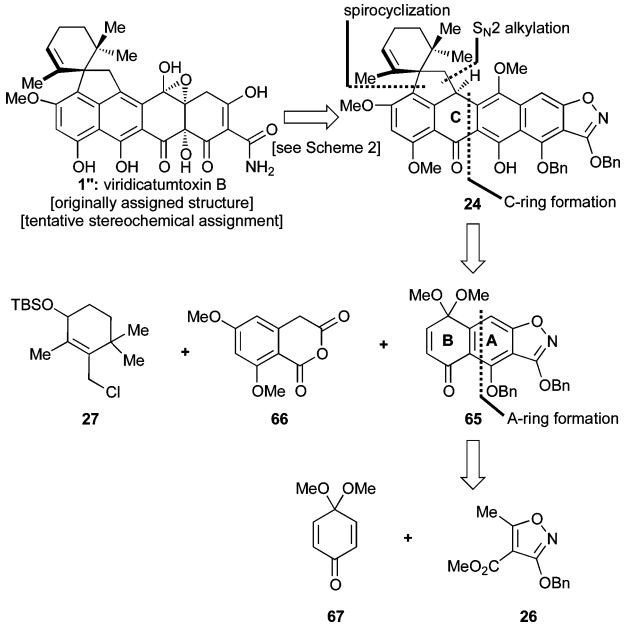

Scheme 8. Synthesis and 1,2-Addition of Stork–Hagedorn Isoxazole 26 to Quinone Monoketal 67[a]

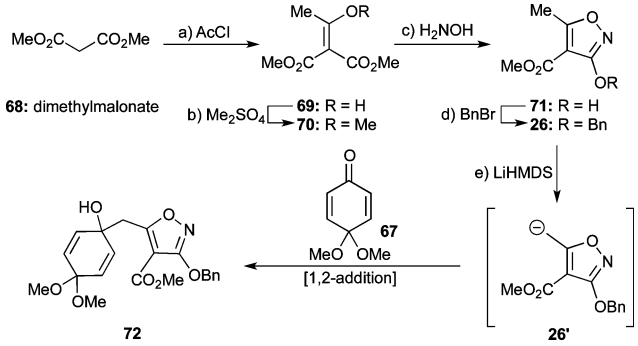

[a]Reagents and conditions: (a) $MgCl_2$ (1.0 equiv), Et_3N (2.0 equiv), AcCl (1.0 equiv), MeCN, 0 → 25 °C, 23 h, 96%; (b) Me_2SO_4 (1.3 equiv), K_2CO_3 (1.3 equiv), DMF, 0 → 25 °C, 17 h, 54%; (c) H_2NOH·HCl (1.4 equiv), NaOMe (3.1 equiv), MeOH, 0 → 25 °C, 24 h, 48%; (d) BnBr (1.2 equiv), Ag_2O (1.5 equiv), DMF, 25 °C, 18 h, 67%; (e) LiHMDS (1.4 equiv), THF, −78 °C, 40 min; then **67** (1.0 equiv), −78 → −30 °C, 45 min, 62%. Ac = acetyl, DMF = dimethylformamide, HMDS = hexamethyldisilazide.

undesirable due to safety concerns. With isoxazole **26** readily available, we next attempted its conjugate addition to quinone monoketal **67**, as shown in Scheme 8. Thus, deprotonation of the methyl group of **26** with LiHMDS, followed by addition of quinone monoketal **67** to the resulting anion (**26′**), however, led to 1,2-addition product **72**, rather than the desired 1,4-product.

Faced with this predicament, we decided to install an electron-withdrawing group at the isoxazole methyl group, which we hoped would make the resulting nucleophile softer due to its vinylogous diketone nature.[18a] Toward that end, and as shown in Scheme 9, treatment of isoxazole **26** with LiHMDS followed by quenching with methyl chloroformate provided **73** (96% yield). Michael addition of the latter to quinone

Scheme 9. First Synthesis of AB-Quinone Monoketal 65[a]

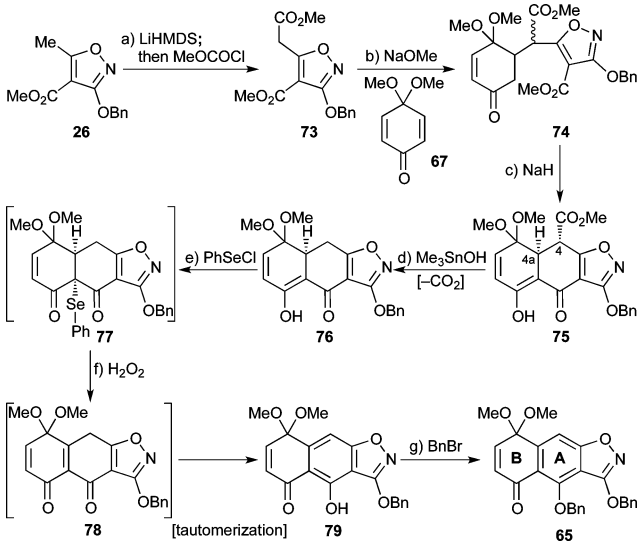

[a]Reagents and conditions: (a) LiHMDS (2.2 equiv), THF −78 °C, 30 min; then MeOCOCl (1.0 equiv), −78 °C, 45 min, 96%; (b) **67** (1.0 equiv), NaOMe (1.0 equiv), MeOH, 25 °C, 18 h, 71%, ca. 3:1 dr; (c) NaH (3.9 equiv), toluene, 0 → 90 °C, 2.5 h; (d) Me_3SnOH (9.0 equiv), $ClCH_2CH_2Cl$, 80 °C, 21 h, 39% for two steps; (e) PhSeCl (1.9 equiv), py (2.1 equiv), CH_2Cl_2, 0 °C, 1.5 h; (f) H_2O_2 (excess), CH_2Cl_2, 0 °C, 54% for two steps; (g) BnBr (3.0 equiv), K_2CO_3 (4.0 equiv), acetone, 25 → 60 °C, 6.5 h, 94%. py = pyridine.

monoketal **67** was then achieved under basic conditions (NaOMe) to give adduct **74** in 71% yield as an inconsequential ca. 3:1 mixture of diastereomers. Dieckmann condensation within **74** induced by NaH then led to tricycle **75** as a single diastereomer ($^3J_{4,4a}$ = 11.2 Hz), presumably through epimerization at C4 during the reaction. Demethylation and subsequent decarboxylation of **75** was then carried out with Me_3SnOH[49] at elevated temperatures, providing **76** in 39% yield for the two steps. Of note here is the observation that the use of LiOH proved unsuccessful in promoting this transformation. Subsequent oxidation of the latter substrate (i.e., **76**) by way of selenide formation/oxidation/syn-elimination furnished compound **79** (54% for the two steps), through intermediate **77** and transient species **78**. Finally, benzylation of the free phenolic moiety within **79** (BnBr, K_2CO_3, 94%) afforded the desired AB-ring system fragment **65** (mp = 103 °C, Et_2O). The structure of this key intermediate was unambiguously confirmed by X-ray crystallographic analysis (see ORTEP representation, Figure 1).

While the above route provided sufficient quantities of fragment **65** for preliminary studies, scaling up the synthetic sequence, especially the ester saponification with Me_3SnOH, proved inconvenient. To circumvent this problem, we elected to change the C4-ester group to a more labile one. Alternative moieties considered were the ethoxyethyl ester, originally employed by Stork,[18a] and the cyclic anhydride **80** (see Scheme 10), which was envisioned to undergo a one-pot Michael–Dieckmann/decarboxylation cascade sequence. Eventually, however, we selected a Teoc ester due to its anticipated orthogonality to the rest of the functionalities within the molecule. Thus, and as shown in Scheme 10, installation of the Teoc ester at C4 of isoxazole **26** was accomplished using a similar protocol as for the methyl ester (LiHMDS; then TeocCl, 88%) to afford derivative **81**. Michael reaction of the

dx.doi.org/10.1021/ja506472u | J. Am. Chem. Soc. 2014, 136, 12137–12160

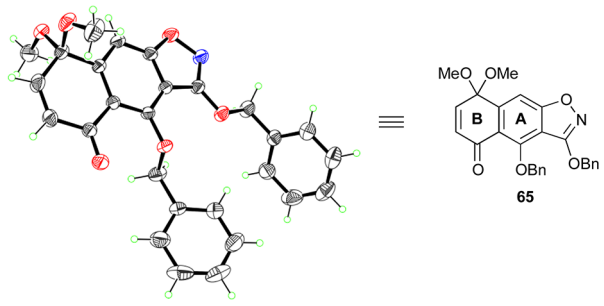

Figure 1. ORTEP representation of AB-quinone monoketal **65**. Thermal ellipsoids at 30% probability. Gray = carbon, red = oxygen, blue = nitrogen, green = hydrogen.

Scheme 10. Improved Synthesis of AB-Quinone Monoketal 65 through the Use of a Teoc Ester[a]

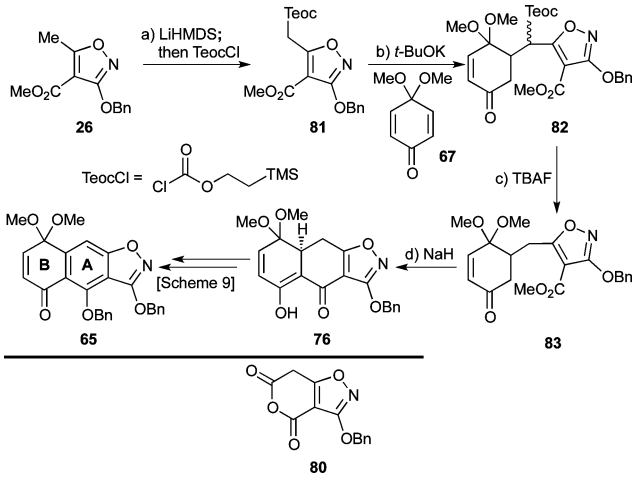

[a]Reagents and conditions: (a) LiHMDS (2.2 equiv), THF, −78 °C, 30 min; then TeocCl (1.1 equiv), −78 °C, 1 h, 88%; (b) **67** (1.0 equiv), *t*-BuOK (0.2 equiv), toluene, 25 °C, 4 h, 71%, ca. 2.4:1 dr; (c) TBAF (1.2 equiv), THF, 25 °C, 45 min, 85%; (d) NaH (4.0 equiv), toluene, 0 → 110 °C, 4 h, 80%. TBAF = tetra-*n*-butylammonium fluoride.

latter with **67** (*t*-BuOK) then gave adduct **82** (71% yield, ca. 2.4:1 dr, inconsequential). At this point, it was gratifying to observe that the Teoc group could be removed in a straightforward fashion using TBAF at 25 °C to furnish decarboxylated product **83** (85% yield). Dieckmann cyclization within **83**, again induced by NaH, provided intermediate **76** (80% yield) which intersected the previously described route to **65** (see Scheme 9).

With AB-enone **65** in hand, our attention turned toward the synthesis of the desired ABCD-ring fragment **88** (Scheme 12) through union of the former with a suitable CD-ring precursor. Due to the observed 1,2-addition of isoxazole anion **26′** to quinone monoketal **67** (see Scheme 8), we anticipated the need for a soft CD-ring nucleophile. Toward this end, we selected the known homophthalic anhydride **66** [readily prepared in four steps from 4-chlororesorcinol (**84**) through intermediate **85** as shown in Scheme 11].[45] Anhydride **66** has traditionally been used (after deprotonation with a strong base, typically NaH or LDA) in Tamura-type Diels–Alder reactions with quinones.[50] However, we found that substrate **66** could be united with AB-enone **65** using DBU as the base at 60 °C to afford pentacyclic system **88** (82% yield, see Scheme 12). A ^{1}H NMR-tube experiment to monitor the reaction between **65** and

Scheme 11. Preparation of Cyclic Anhydride Fragment 66[a]

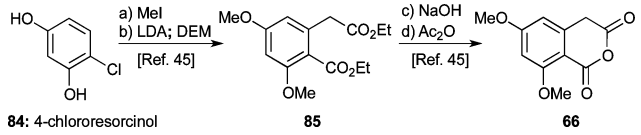

[a]Reagents and conditions: (a) MeI (4.0 equiv), K_2CO_3 (8.0 equiv), acetone, reflux, 15 h, 91%; (b) NaH (6.0 equiv), diethyl malonate (4.0 equiv), THF, 0 °C, 2.5 h; then LDA (1.0 equiv), THF, 0 °C, 3.5 h, 65%; (c) MeOH:2 M NaOH 1:1, reflux, 12 h, 97%; (d) Ac_2O (4.2 equiv), toluene, reflux, 2 h, 99%. DEM = diethyl malonate.

Scheme 12. Synthesis of Intermediate 88 through a Michael–Dieckmann/Decarboxylation Cascade Sequence and Spirocyclization of Hexacycle 90 to Heptacycle 24[a]

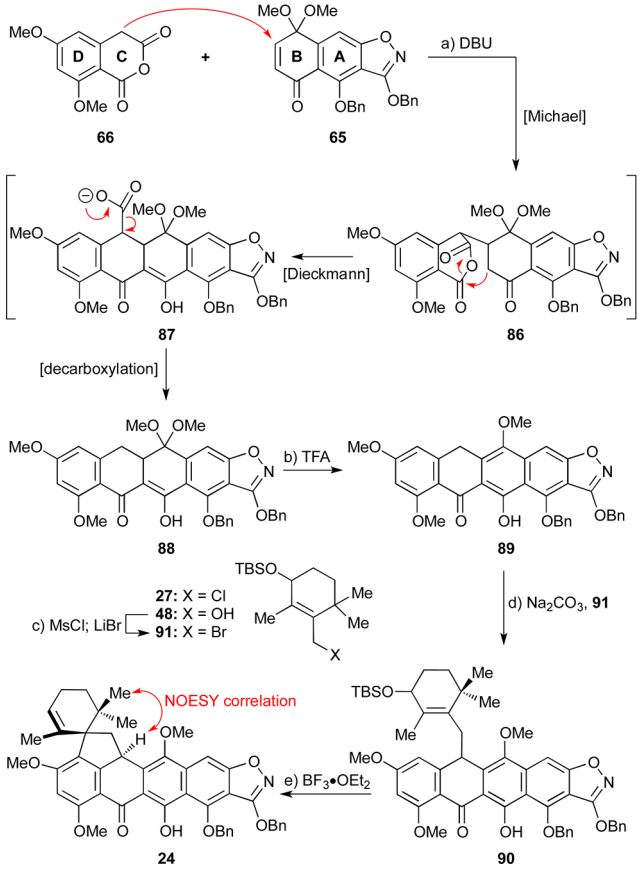

[a]Reagents and conditions: (a) **65** (1.0 equiv), DBU (3.0 equiv); then **66** (1.3 equiv), MeCN, 25 → 60 °C, 18 h, 82%; (b) TFA (4.9 equiv), CH_2Cl_2, 25 °C, 20 min, quant; (c) Et_3N (2.0 equiv), MsCl (1.7 equiv), CH_2Cl_2, −50 °C, 1 h; then LiBr (3.5 equiv), THF, −50 → −20 °C, 1 h, quant; (d) **91** (1.5 equiv), Na_2CO_3 (9.1 equiv), DMF, 25 °C, 45 min, 78%, ca. 6:1 dr; (e) BF_3·OEt_2 (0.6 equiv), CH_2Cl_2, 0 °C, 1 h, 55%. DBU = 1,8-diazabicyclo[5.4.0]undec-7-ene, TFA = trifluoroacetic acid.

66 suggested that it proceeds via a distinct stepwise mechanism (intermediates **86** and **87** were tentatively observed; see selected peaks, Figure 2), as opposed to a concerted [4 + 2] cycloaddition followed by decarboxylation. Additionally, this experiment indicated that the reaction required approximately 20 h for completion. Elimination of methanol from cyclization product **88**, induced by exposure to TFA in CH_2Cl_2, then led to elaborated anthrone **89** in quantitative yield.

dx.doi.org/10.1021/ja506472u | J. Am. Chem. Soc. 2014, 136, 12137–12160

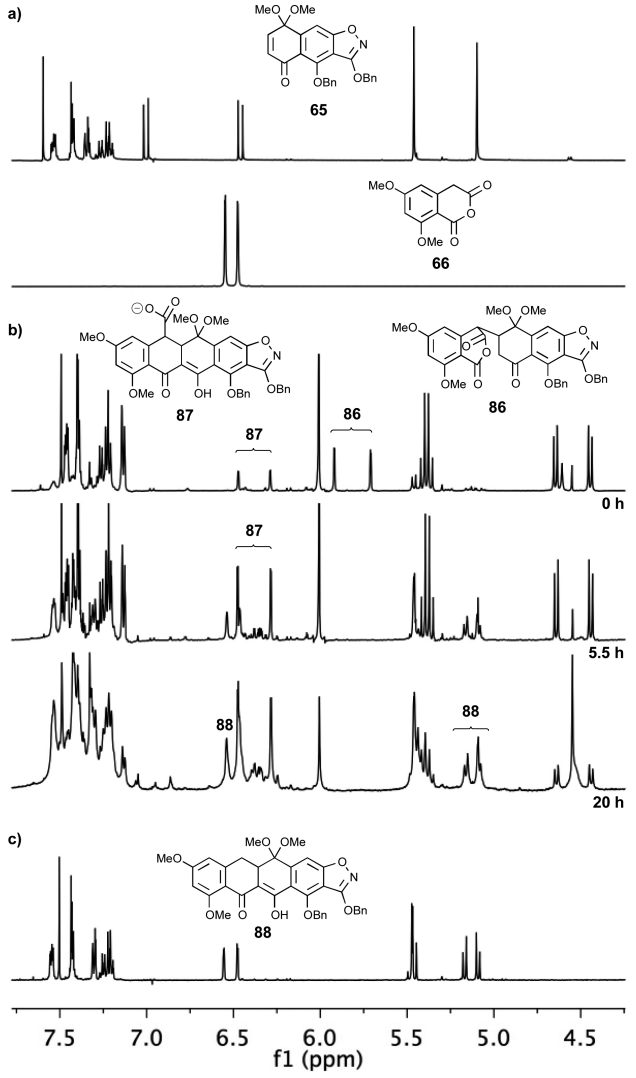

Figure 2. Monitoring the coupling of cyclic anhydride **66** and AB-quinone monoketal **65** by ^{1}H NMR spectroscopy (MeCN-d_3, 500 MHz): (a) ^{1}H NMR spectra of starting materials **65** and **66**; (b) ^{1}H NMR spectra during reaction (0, 5.5, and 20 h); (c) ^{1}H NMR spectrum of product **88** after purification.

Attempts to alkylate anthrone **89**, however, with chloride **27** (Scheme 12) under the conditions employed for the alkylation of the simpler anthrone **28** (Scheme 5) were thwarted by the insolubility of **89** in acetone and the low reactivity of **27**, necessitating a search for a new protocol to achieve the desired union of the two partners. Thus, with further experimentation, it was found that upon using the corresponding allylic bromide **91** (prepared from allylic alcohol **48** by treatment with MsCl, Et_3N, and LiBr in quantitative yield, Scheme 12) and changing the solvent from acetone to DMF, the required alkylation proceeded smoothly at ambient temperature and within 1 h to provide the desired coupling product **90** in 78% yield.

With intermediate **90** available, and in an effort to prepare subtarget **24** (Scheme 12), we then proceeded to apply our original spirocyclization conditions (i.e., ZnI_2, CH_2Cl_2, reflux, see Scheme 5), but unfortunately encountered side-products, presumed to arise from elimination,[51] demethylation,[52] and/or benzylic oxidation reactions. We reasoned that such side reactions could be suppressed by using a nonmobile counterion on the activating agent, a hypothesis that prompted us to test $BF_3{\cdot}OEt_2$, a catalyst that held promise to also induce the pending spirocyclization at lower temperatures. Indeed, exposure of **90** to substoichiometric amounts of this Lewis acid at 0 °C led to the formation of the desired heptacycle **24** in 55% yield with minimum amounts of side-products. The configuration of **24** was confirmed as shown in Scheme 12 by NOESY experiments.

Scheme 13 depicts our attempts to realize the singlet oxygen cascade sequence from **93** (derived from **24** via benzoate

Scheme 13. Preparation of Endoperoxide Precursor 93 and Expected Pathway to Oxygenated Species 97[a]

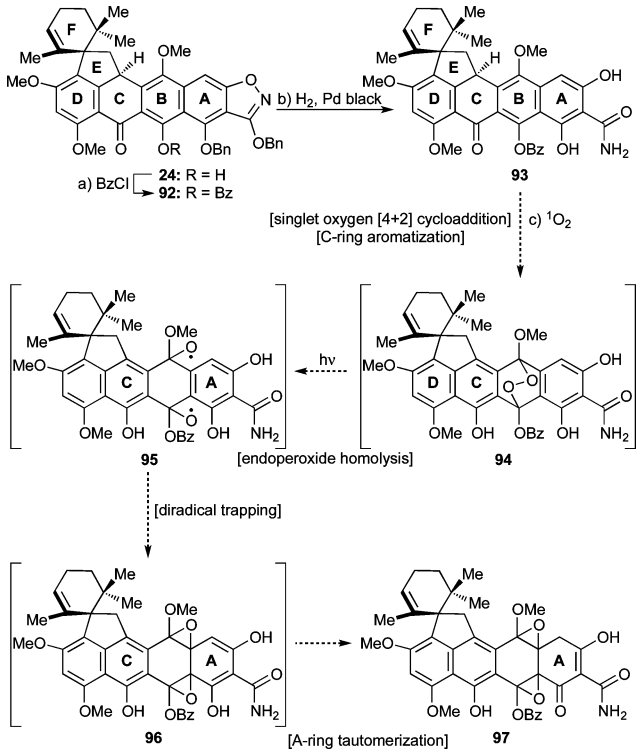

[a]Reagents and conditions: (a) BzCl (15 equiv), Et_3N (25 equiv), DMAP (0.06 equiv), CH_2Cl_2, 25 °C, 45 min, 79%; (b) Pd black (5.0 equiv), 1,4-dioxane:MeOH 1:1, H_2, 25 °C, 20 min, quant; (c) O_2, TPP (cat.), CH_2Cl_2, sun lamp, −78 °C. Bz = benzoyl, TPP = tetraphenylporphyrin.

derivative **92**) to **97** through postulated intermediates **94**–**96**. Thus, heptacyclic phenol **24** was converted to its benzoate **92** (BzCl, Et_3N, 79% yield) and thence to hexacyclic system **93** through hydrogenolysis (Pd black, H_2, quantitative yield) of the N–O bond and the two benzyl ether moieties. Our reasoning for the protection of the phenolic group of **24** was based on the assumption that this change would promote the aromatization of ring C within **92** by removing the possibility for a H-bond to the C-ring carbonyl group. This assumption, however, proved erroneous, as both **92** and **93** were found to exist exclusively in their C-ring keto forms as opposed to their enol (phenolic) forms. In retrospect, this outcome is not surprising in light of previous reports, which indicated that conjugation of a naphthalene ring (as in **92** and **93**) with a ketone provides thermodynamic stability greater than that of its phenolic counterpart (as in the phenolic tautomers of **92** and **93**).[53]

Anticipating the singlet oxygen-initiated cascade sequence of reactions shown in Scheme 13 (**93** → **94** → **95** → **96** → **97**) based on precedented chemistry[29] (see Scheme 3), we

dx.doi.org/10.1021/ja506472u | J. Am. Chem. Soc. 2014, 136, 12137–12160

proceeded to react substrate **93** with singlet oxygen. This transformation, however, could not be realized. Thus, bubbling of O_2 through a solution of substrate **93** in CH_2Cl_2 in the presence of catalytic quantities of TPP and with sun lamp irradiation at −78 °C rapidly produced a product that proved, upon warming, too labile for characterization. Prolonged irradiation at −78 °C produced no detectable amounts of bis-epoxide **97**. We then attempted to tautomerize the C-ring of **93** to its corresponding phenolic form under basic conditions with the hope that this maneuver (see above, Scheme 6) might lead to a favorable result in the singlet oxygen reaction. However, the previous conditions used for the corresponding keto−phenol tautomerization (**25** → **63**, K_2CO_3, MeOH, Scheme 6) failed to yield the desired product. Other efforts to achieve the desired outcome included attempts to form and rearrange the endoperoxide using different sensitizers on substrates with and without the isoxazole ring, the latter scenario being inspired by Myers's hypothesis that the isoxazole moiety may act as a self-sensitizer.[20a] These experiments failed to produce any of the proposed intermediates in Scheme 13 (i.e., **94**−**97**).

On the basis of these findings, we were forced to explore alternative phenolic oxidation protocols in an effort to install oxidation at C12a (Scheme 14). Attempted phenolic oxidations of substrate **24**, or its corresponding hydrogenolyzed counterpart **98**, were unsuccessful. A number of other conditions, including hypervalent iodine reagents, Fremy's salt, $Pb(OAc)_4$, and various metals with molecular oxygen, were also unsuccessful. Typically either no reaction was observed or the substrate decomposed, especially for the more electron-rich substrate **98**. Furthermore, phenol **101** was synthesized as a possible substrate for C12a hydroxylation through a sequence involving PIFA oxidation to the quinone, benzoyl ester formation (BzCl, 65% for two steps), and regioselective debenzylation ($MgBr_2{\cdot}OEt_2$, 75%). Phenolic oxidation of this substrate (i.e., **101**), however, also failed to produce the desired C12a oxidation product **102**. The challenges faced here with respect to installation of the C12a hydroxyl group are reminiscent of previous synthetic efforts toward tetracyclines, including those of Woodward,[13] Muxfeldt,[15] Stork,[18] and, in particular, Barton.[54]

The failure to install the obligatory hydroxyl groups at C4a and C12a through dearomatization pathways refocused our attention on alternative tactics, the choice of which was based on the intelligence gathered thus far. This information pointed away from an aromatic A-ring as a precursor to the desired oxygenation.

Third-Generation Approach: Stepwise Strategies To Install the C4a and C12a Hydroxyl Groups. Our first attempts to install the coveted hydroxyl groups onto the substrate via enol or enolate chemistry focused on the rather simple AB-ring fragment **76** (Scheme 15). As shown in this scheme, treatment of **76** with DMDO gave a mixture of C12a-hydroxylated compounds **103** and 12a-*epi*-**103** (ca. 3:5 ratio, 79% yield combined, chromatographically separated, inconsequential) whose configurations were established through analysis of their NOESY correlations and $^{2,3}J$ coupling constants (see structure 12a-*epi*-**103**). We envisioned that the extrusion of methanol from **103** might result in the formation of methyl enol ether **105**, whose selective epoxidation would furnish **106**. Such a strategy would be conceptually similar to that of Myers, which features a fully functionalized AB-ring enone system. However, the elimination of methanol (**103** → **104** → **105**, Scheme 15) turned out to be surprisingly problematic. A variety of Lewis- or Brønsted-acidic conditions failed to promote this transformation, leading instead to various decomposition side-products, including lactone ring expansion products involving the C12a hydroxyl group. We reasoned that these failures may be due to mismatched electronics which did not allow for the formation of the oxonium moiety adjacent to

Scheme 14. Phenolic Oxidation Attempts To Hydroxylate at C12a Heptacycle 24 and Derivatives 98 and 101[a]

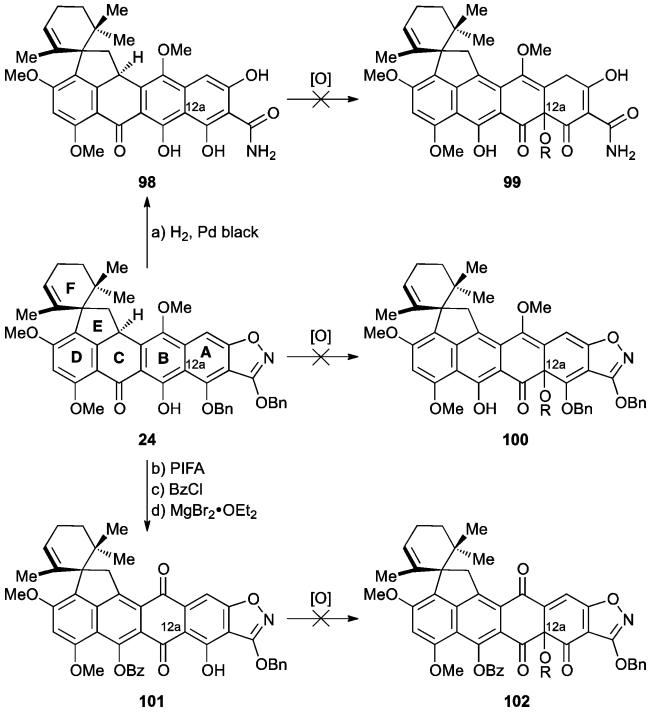

[a]Reagents and conditions: (a) Pd black (5.0 equiv), H_2, 1,4-dioxane:MeOH, 1:1, 25 °C, 30 min, quant.; (b) PIFA (1.1 equiv), DMF:H_2O 9:1, 40 °C, 2 h; (c) BzCl (4.4 equiv), Et_3N (10 equiv), DMAP (0.06 equiv), CH_2Cl_2, 25 °C, 5 min, 65% for two steps; (d) $MgBr_2{\cdot}OEt_2$ (1.0 equiv), Et_2O:benzene 1:7, 25 °C, 2 h, 75%. PIFA = phenyliodonium bis(trifluoroacetate).

Scheme 15. Early Stage Installation of the C12a Hydroxyl Group and Failed Attempts To Install Oxygenation at C4a[a]

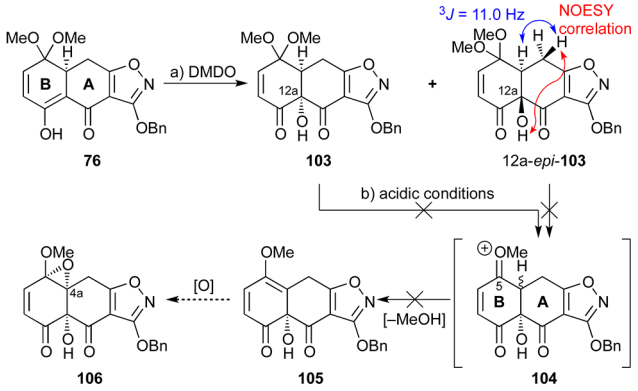

[a]Reagents and conditions: (a) DMDO (1.7 equiv), acetone:H_2O 9:1, 25 °C, 1.5 h, 29% for **103**, 50% for 12a-*epi*-**103**; (b) conditions included several Lewis and Brønsted acids. DMDO = dimethyldioxirane.

dx.doi.org/10.1021/ja506472u | J. Am. Chem. Soc. 2014, 136, 12137−12160

the enone system. We then speculated that the presence of an aromatic ring adjacent to the oxonium system (see structure **104**, Scheme 15) might facilitate the formation of such a species.

With these postulates in mind, a new strategy was devised based on the retrosynthetic analysis shown in Scheme 16,

Scheme 16. Third-Generation Retrosynthetic Analysis of Viridicatumtoxin B Structure 1″

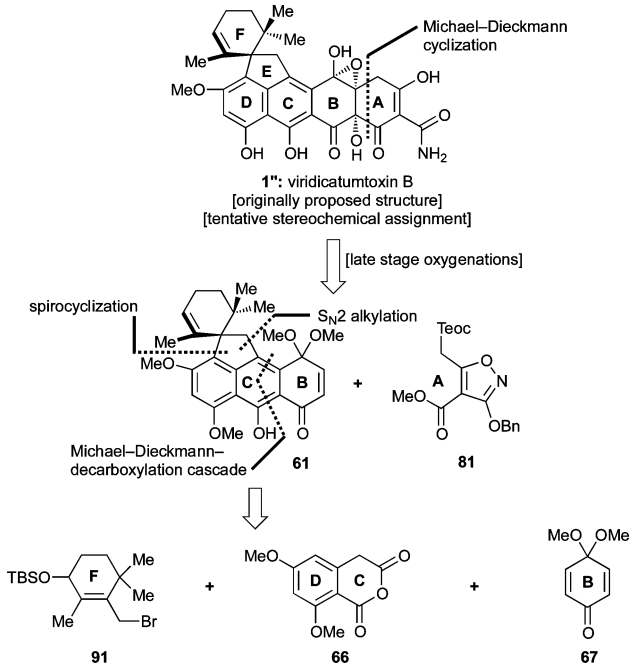

which most notably circumvents an aromatic A-ring and postpones the C4a/C12a oxygenations to the later stages of the projected synthesis. Thus, viridicatumtoxin B structure **1″** was disconnected through the A-ring with a Michael−Dieckmann reaction similar to that which had successfully been deployed in the second-generation strategy. This analysis unveiled isoxazole fragment **81** and BCDEF pentacycle **61** as potential key building blocks. The latter was envisioned to be derived from fragments **91**, **66**, and **67** through a pathway similar to that of the second-generation approach involving homophthalic anhydride/quinone monoketal cyclization, anthrone alkylation, and Lewis acid-mediated spirocyclization (see Scheme 12).

As shown in Scheme 17, a similar set of reaction conditions as those used to prepare **24** (see Scheme 12) were employed to synthesize spirocyclic compound **60**. Thus, DBU-promoted Michael−Dieckmann/decarboxylation cascade (**107**, 50% yield) and CSA-catalyzed aromatization (quant.) gave anthrone **108**. Anthrone alkylation with the allylic bromide **91** then gave the alkylated compound **109** (75%, ca. 1:1 dr, inconsequential). The steric congestion around the newly generated C−C bond of the latter compound manifested itself in some unusual NMR spectroscopic features. Thus, all three methyl groups of the F-ring in **109** showed very broad signals, which suggested hindered rotation around this region of the molecule at 298 K, thereby forcing the methyl groups to experience a number of different magnetic environments. Supporting this notion was the fact that when the ^{1}H NMR spectrum of **109** was acquired at 338 K in DMSO-d_6, the methyl signals sharpened considerably. Spirocyclization of **109** proceeded in the presence

Scheme 17. Synthesis of BCDEF Pentacycle 60[a]

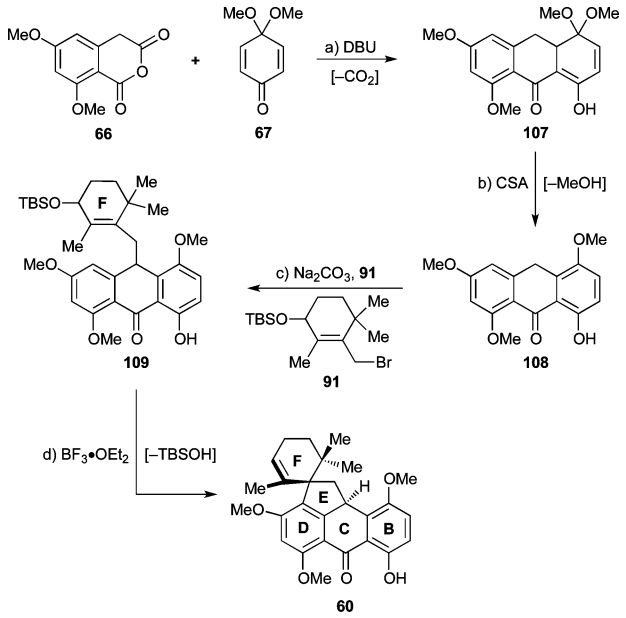

[a]Reagents and conditions: (a) **66** (1.0 equiv), **67** (3.0 equiv), DBU (3.0 equiv), MeCN, 60 °C, 15 h, 50%; (b) CSA (0.02 equiv), CH_2Cl_2, 25 °C, 30 min, quant.; (c) **91** (1.2 equiv), Na_2CO_3 (10 equiv), DMF, 25 °C, 1 h, 75%, ca. 1:1 dr; (d) BF_3·OEt_2 (0.2 equiv), CH_2Cl_2, 0 °C, 20 min, 82%. CSA = (±)-camphor-10-sulfonic acid.

of BF_3·OEt_2 as before, producing the desired pentacyclic compound **60** in 82% yield. An X-ray crystallographic analysis of **60** [mp = 114−116 °C (EtOAc:$CHCl_3$ 1:1), see ORTEP, Figure 3] unambiguously proved its spectroscopically derived structural assignment.[55]

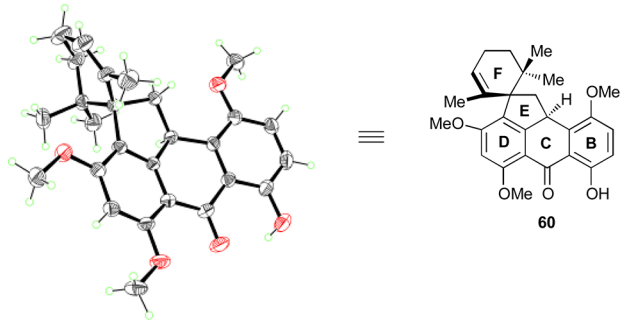

Figure 3. ORTEP representation of spirocycle **60**. Thermal ellipsoids at 30% probability. Gray = carbon, red = oxygen, green = hydrogen.

With key intermediate **60** now accessible, we turned next to its phenolic oxidation. Although initially concerned, due to the previous recalcitrance of substrate **25** (see Scheme 6) to undergo phenolic oxidation, these trepidations proved to be unfounded.

Thus, in an initial experiment, treatment of spirocycle **60** with PIDA (3.0 equiv) led to the formation of desired quinomethide−quinone monoketal **111** (54% yield) and side-product **112** (22%, Scheme 18). The stereochemical configuration of the latter species was initially assigned on the basis of a NOESY experiment and was later unambiguously confirmed through X-ray crystallographic analysis [mp = 201−203 °C (EtOAc:CH_2Cl_2 1:1), see ORTEP representation, Figure 4].

dx.doi.org/10.1021/ja506472u | J. Am. Chem. Soc. 2014, 136, 12137−12160

Scheme 18. Optimization of Phenolic Oxidation of Substrate 60 to *p*-Quinomethide 111[a]

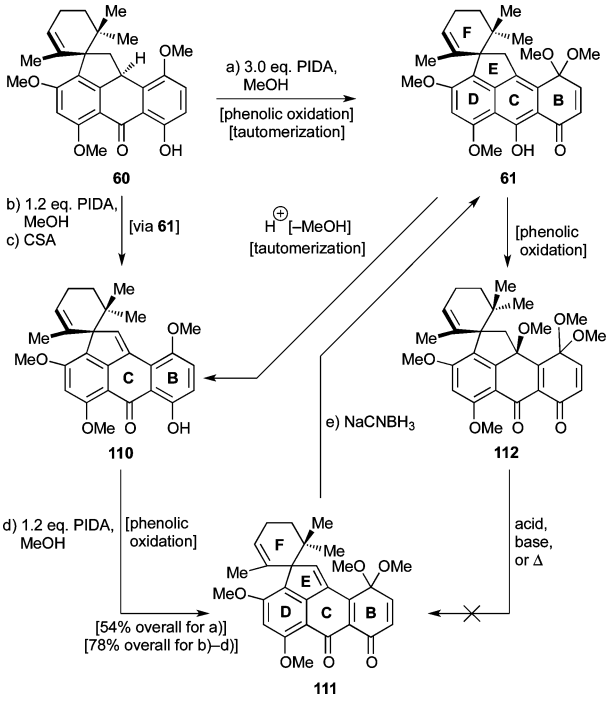

[a]Reagents and conditions: (a) $PhI(OAc)_2$ (3.0 equiv), MeOH, 25 °C, 2.8 h, 54% for **111** + 22% for **112**; (b) $PhI(OAc)_2$ (1.2 equiv), MeOH:CH_2Cl_2 1:1, 0 → 25 °C, 1 h; (c) CSA (0.07 equiv), CH_2Cl_2, 0 °C, 30 min; (d) $PhI(OAc)_2$ (1.2 equiv), MeOH, 25 °C, 1.5 h, 78% overall for b, c, and d; (e) $NaCNBH_3$ (1.2 equiv), MeOH, 0 → 25 °C, 45 min, 29%, unoptimized.

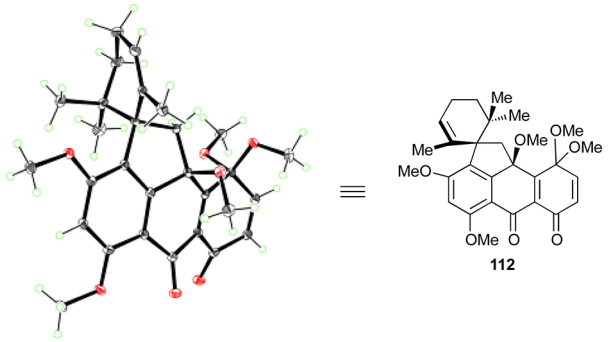

Figure 4. ORTEP representation of side-product **112**. Thermal ellipsoids at 30% probability. Gray = carbon, red = oxygen, green = hydrogen.

The formation of both **111** and **112** in the presence of excess PIDA in MeOH at 25 °C is apparently a consequence of the competing pathways shown in Scheme 18. Thus, initial phenolic oxidation of **60** affords **61**, which suffers elimination of MeOH induced by the in situ-generated AcOH leading to phenol *p*-quinomethide **110** (isolated and characterized), whose phenolic oxidation furnishes **111**. Intermediate **61**, however, may also undergo phenolic oxidation, furnishing **112**. The facility by which substrate **60** undergoes phenolic oxidation as compared to its simpler counterpart **25** mentioned above (see Scheme 6) is attributed to the extra methoxy group residing on ring B of the former. Attempts to convert side-product **112** to the desired compound **111** under acidic, basic, or thermal conditions failed.

Efforts to optimize the conversion of **60** to **111** led to the preferred three-step sequence (via **61** and **110**) shown in Scheme 18. Thus, employment of limited quantities of PIDA (1.2 equiv), MeOH:CH_2Cl_2 (1:1) as solvent, and lower temperature (0 → 25 °C), generated intermediate **61** in high yield. The crude product in CH_2Cl_2 was then treated with catalytic quantities of CSA at 0 °C to provide *p*-quinomethide **110**, which was subjected to further phenolic oxidation with PIDA in MeOH to afford **111** in 78% overall yield for the three steps. It should be mentioned here that substrate **61** proved intransigent to the desired pending reactions (i.e., Michael–Dieckmann cascade), leading instead to MeOH-elimination product **110**. Access to substrate **111** opened the way forward, despite the need for reduction of the *p*-quinomethide to the desired phenolic structural motif at a later stage. The feasibility of such a transformation was briefly explored at this stage, leading to the finding that it could be achieved with $NaCNBH_3$ (Scheme 18, **111** → **61**, 29% yield, unoptimized).

The next task was the union of pentacyclic enone **111** with isoxazole **81** through the Michael–Dieckmann sequence of reactions as indicated in Scheme 19. On the basis of our success with this sequence on the simpler systems discussed above (i.e., Schemes 9 and 10), we were rather optimistic for favorable results in this instance as well. However, initial experimentation with methyl ester **81** as the isoxazole equivalent proved

Scheme 19. Failed Attempts To Close the A-Ring through Dieckmann Condensations[a]

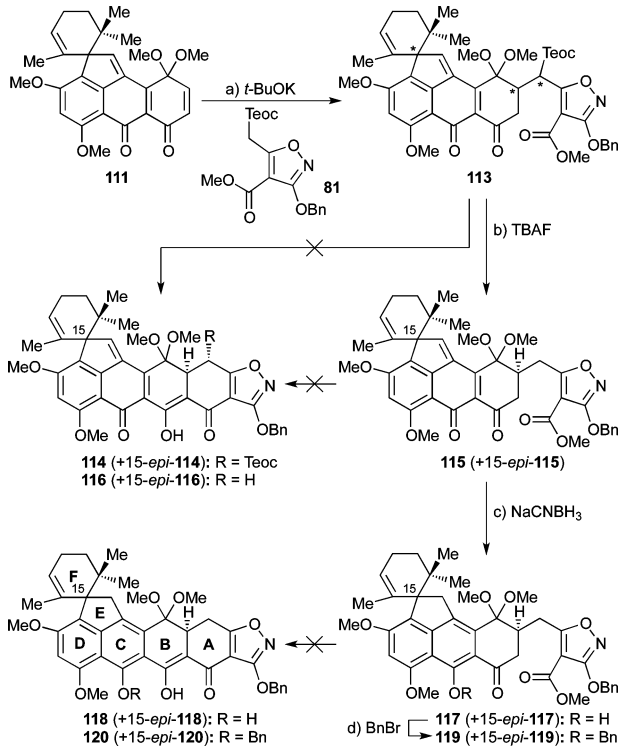

[a]Reagents and conditions: (a) **81** (1.1 equiv), *t*-BuOK (0.2 equiv), toluene, 25 °C, 45 min, 74%, mixture of four diastereomers; (b) TBAF (1.2 equiv), THF, 25 °C, 10 min, 60%, ca. 2:1 dr; (c) $NaCNBH_3$ (5.0 equiv), THF, 0 °C, 2 min, 82%, ca. 2:1 dr; (d) BnBr (10 equiv), NaH (10 equiv), TBAI (0.15 equiv), toluene, 25 → 100 °C, 3.75 h, 85%, ca. 2:1 dr. TBAI = tetra-*n*-butylammonium iodide.

dx.doi.org/10.1021/ja506472u | J. Am. Chem. Soc. 2014, 136, 12137–12160

otherwise. Thus, although the first step (Michael reaction, Scheme 19) of the anticipated fusion of **111** with **81** proceeded well, leading to Michael adduct **113** (*t*-BuOK cat., 74% yield, mixture of four diastereoisomers), conditions for the subsequent step (Dieckmann reaction) proved elusive despite considerable experimentation (a variety of basic conditions typically led to recovery of unreacted **113** or decomposition). Removal of the Teoc group from **113** led to **115** and its C15-epimer (15-*epi*-**115**, ca. 2:1 dr)[56] (TBAF, 60% yield), which, however, also failed to undergo the coveted Dieckmann cyclization (to **116**, Scheme 19). Reduction of the quinomethide moiety of **115**/15-*epi*-**115** furnished **117**/15-*epi*-**117** ($NaCNBH_3$, 82% yield, ca. 2:1 dr). The dibenzyl ether (**119**/15-*epi*-**119**) of the latter was also prepared (NaH, BnBr, TBAI cat., 85% yield, ca. 2:1 dr). Neither **117**/15-*epi*-**117** nor **119**/15-*epi*-**119** entered the desired Dieckmann reaction to afford the expected heptacyclic systems **118**/15-*epi*-**118** or **120**/15-*epi*-**120**, respectively. Similar problems were reported by Stork and Kahne.[57]

Faced with these difficulties and inspired by the work of White[58] and Myers,[20d] we opted to employ the phenyl ester counterpart of isoxazole **81** (see **123**, Scheme 20a). Isoxazole

Scheme 20. Synthesis of Phenyl Ester 123 (a) and Its Successful Michael–Dieckmann Cyclization with Enone 111 (b)[a]

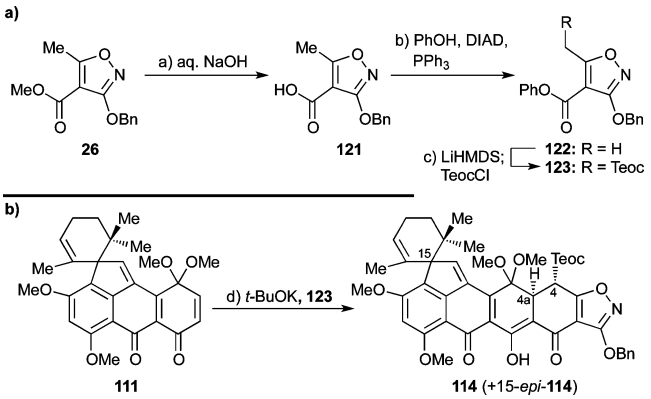

[a]Reagents and conditions: (a) NaOH (1.9 equiv), H_2O:EtOH 3:10, 25 °C, 3 h, 99%; (b) PPh_3 (1.05 equiv), PhOH (1.05 equiv), DIAD (1.05 equiv), THF, reflux, 3 h, 78%; (c) LiHMDS (2.2 equiv), THF, −78 °C, 30 min; then TeocCl (2.2 equiv), −78 °C, 2 h, 86%; (d) **123** (1.1 equiv), *t*-BuOK (1.2 equiv), toluene, 25 °C, 15 min, 94%, ca. 1:1 dr. DIAD = diisopropyl azodicarboxylate.

phenyl ester **123** was prepared from methyl ester **26** via **121** and **122** through saponification (NaOH, 99% yield), esterification with PhOH under Mitsunobu conditions (PPh_3, DIAD, 78% yield),[59] and Teoc attachment (LiHMDS, TeocCl, 86% yield) as shown in Scheme 20a. It is of note that several standard ester-forming reactions (e.g., mixed anhydride, acid chloride, DCC) failed to bring about the desired esterification between **121** and PhOH. Gratifyingly, quinone monoketal **111** reacted smoothly with phenyl ester isoxazole **123** in the presence of a slight excess of *t*-BuOK to give directly the desired heptacyclic compound **114** as a ca. 1:1 mixture with its C-15 diastereoisomer (15-*epi*-**114**) in 94% yield (Scheme 20b).[60] The stereochemical relationship of H4 and H4a within **114** was evident from the observed coupling constant $^3J_{4,4a}$ = 9.9 Hz, indicative of the diaxial disposition of these protons. The impressive rapidity (<15 min at 25 °C) of the Michael–Dieckmann cascade to afford the heptacyclic product (**111** → **114** + 15-*epi*-**114**) is a testament to the activating power of the phenyl ester moiety in such circumstances.

We initially explored the C12a hydroxylation of substrate **114**, with the Teoc group still intact, as shown in Scheme 21.

Scheme 21. C12a Hydroxylation of Substrate 114[a]

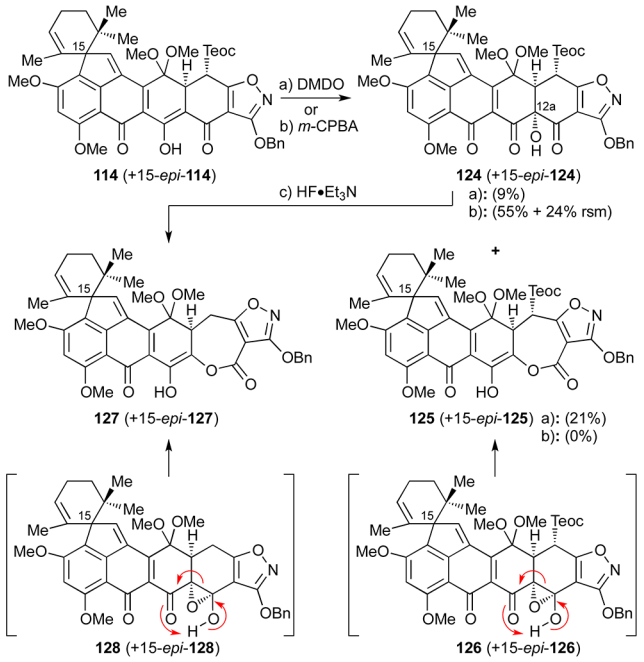

[a]Reagents and conditions: (a) DMDO (2.8 equiv), acetone, −78 °C, 3.5 h, 21% for **125** (ca. 2:1 dr), 9% for **124** (ca. 2:1 dr); (b) *m*-CPBA (2.7 equiv), CH_2Cl_2, −78 °C, 1.5 h, 55% for **124** (71% brsm, ca. 2:1 dr) + 24% recovered **114**; (c) HF·Et_3N (100 equiv), DMSO, 60 °C, 2 h, 43%, ca. 2:1 dr. DMSO = dimethyl sulfoxide.

Thus, hydroxylation of substrate **114** at C12a with DMDO (conditions a) at −78 °C produced the desired compound **124** (together with its C15 epimer 15-*epi*-**124**, ca. 2:1 dr) but only as a minor product (9% combined yield). The major product in this reaction was seven-membered lactone **125** formed together with its C15-epimer (15-*epi*-**125**, 21% combined yield, ca. 2:1 dr) through rearrangement/ring expansion of presumed transient intermediate **126** + 15-*epi*-**126** (see Scheme 21). C12a hydroxylation of substrate **114** + 15-*epi*-**114** was also achieved with *m*-CPBA, this time leading exclusively to the desired hydroxy compound **124** + 15-*epi*-**124** (ca. 2:1 dr) in 71% combined yield based on 24% recovered starting material. However, attempts to remove the Teoc group from the latter mixture with HF·Et_3N led to product **127** + 15-*epi*-**127** from which the Teoc had been removed and the B-ring had been expanded to a seven-membered lactone moiety, presumably through rearrangement of fleeting intermediate **128** + 15-*epi*-**128** (or its Teoc counterpart which suffers Teoc removal concomitantly or subsequently), as depicted in Scheme 21. Exposure of **124** (+ 15-*epi*-**124**) to TBAF led to decomposition and partial recovery of starting material.

The difficulties of removing the Teoc group in the presence of the C12a hydroxyl group led us to explore the alternative sequence in which the Teoc moiety was removed prior to the hydroxylation step. To this end, and as shown in Scheme 22, **114** (+ 15-*epi*–**114**) was treated with excess TBAF in THF, furnishing small amounts of the desired product **116** (+ 15-*epi*-

dx.doi.org/10.1021/ja506472u | J. Am. Chem. Soc. 2014, 136, 12137–12160

Scheme 22. Teoc Removal from 114 and C12a Hydroxylation of 116[a]

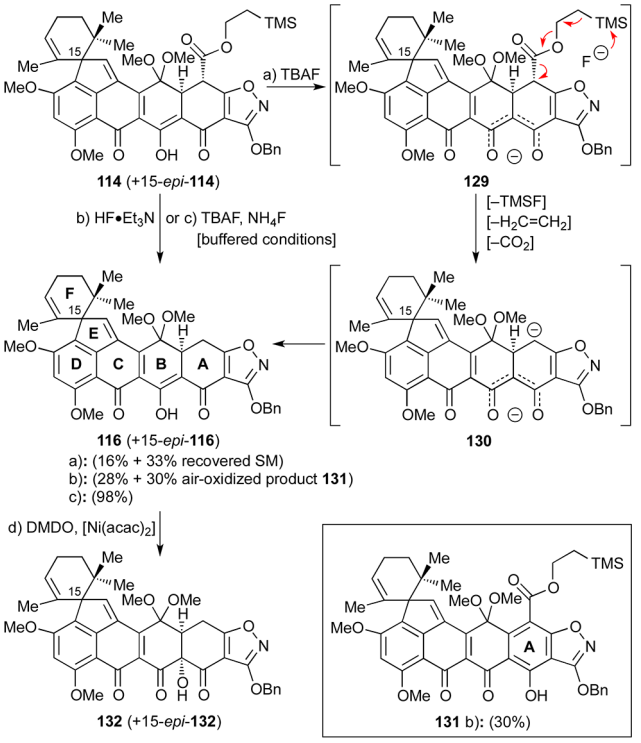

[a]Reagents and conditions: (a) TBAF (5.3 equiv), THF, 25 °C, 1 h, 16% for **116** (ca. 2:1 dr) + 33% recovered **114**; (b) HF·Et_3N (excess), DMSO, 25 → 60 °C, 3 h, 28% for **116** (ca. 2:1 dr) + 30% for **131**; (c) TBAF (10 equiv), NH_4F (20 equiv), THF, 25 °C, 5 min, 98%, ca. 2:1 dr; (d) DMDO (7.6 equiv), $[Ni(acac)_2]$ (0.2 equiv), acetone, −78 → −65 °C, 6.5 h, 61%, ca. 2:1 dr. acac = acetylacetonate.

116, 16% combined yield) and unreacted starting material (33%). Presumably, this failure was caused by deprotonation of the diketone moiety adjacent to the isoxazole (see **129**) that rendered the desired loss of TMSF, ethylene, and carbon dioxide less facile (see **129** → **130**). Faced with this predicament, we undertook a thorough investigation of conditions to achieve the desired Teoc group removal from **114** (+ 15-*epi*-**114**), including $ZnCl_2$, ZnF_2, $MgBr_2$, NH_4F, and SiF_4,[61,62] but unfortunately to no avail. Disappointingly, the use of HF·Et_3N led to the desired product **116** (+ 15-*epi*-**116**) in 28% combined yield, albeit with substantial amounts of side-product **131** (30% yield), presumably formed through an air-oxidation process.[63] Indeed, it was not until we combined Fürstner's TBAF−NH_4F conditions[64] with solvent degassing (to prevent air oxidation of the A-ring) that we reached a solution to this problem, obtaining a pleasing 98% yield of the coveted deprotected product **116** (+15-*epi*-**116**) (Scheme 22).

Having solved the Teoc removal problem, we turned our attention to the C12a hydroxylation task using **116**/15-*epi*-**116** as a substrate. Our initial use of DMDO in acetone at low temperature (i.e., −78 °C) proved irreproducible, gave low conversion to product due to substrate insolubility, and suffered from TLC monitoring problems. To improve the reaction, we resorted to the use of $Ni(acac)_2$, an additive known to facilitate DMDO oxidations through coordination.[65] Indeed, portion-wise addition of DMDO to a stirred mixture of **116**/15-*epi*-**116** and catalytic amounts of $Ni(acac)_2$ in acetone at −78 to −65 °C led to 61% combined yield of C12a hydroxylated product **132**/15-*epi*-**132** (ca. 2:1 dr) as shown in Scheme 22. Both diastereomers were of the syn stereochemical configuration with regard to the C12a hydroxyl and C4a hydrogen residues, presumably as a consequence of the concavity of the AB ring system. It should be noted at this point that at temperatures above −40 °C, epoxidation of the F-ring olefinic site began to occur. Other oxidizing agents such as *m*-CPBA, Davis oxaziridine,[66] and magnesium monoperoxyphthalate (MMPP) proved unsuccessful in providing the desired C12a-hydroxylated compound (i.e., **132** +15-*epi*-**132**).

With the C12a hydroxylation problem solved, the challenge of installing the C4a hydroxyl group became the next task, a mission that was to prove even more intransigent than the one before it. Our initial attempts to achieve this goal are shown in Scheme 23. Thus, reduction of the quinomethide moiety of

Scheme 23. Initial Strategy for C4a Hydroxylation[a]

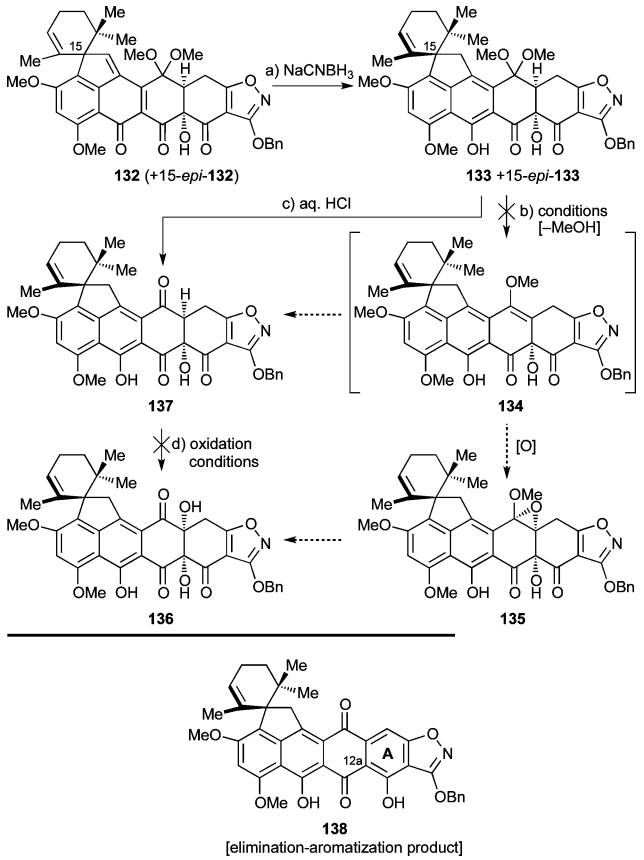

[a]Reagents and conditions: (a) $NaCNBH_3$ (10 equiv), THF, −78 °C, 1.5 h, 51% for **133** + 19% for 15-*epi*-**133**, chromatographically separated; (b) various Lewis and Brønsted acids: see the Supporting Information; (c) THF:2 M aq. HCl 10:1, 25 °C, 3.5 h, 98%; (d) various conditions: see the Supporting Information.

132/15-*epi*-**132** with $NaCNBH_3$ led to the now chromatographically separable derivatives **133** and 15-*epi*-**133**. Gratifyingly, one of the two isomers (more polar) crystallized readily from EtOAc [mp = 213−215 °C (decomp)] and yielded to X-ray crystallographic analysis, establishing its stereochemical configuration as 15-*epi*-**133** (see ORTEP representation, Figure 5), and as a consequence, that of its less polar epimer as the desired diastereomer **133**.[55] Several attempts to prepare methylenol ether **134** as a potential precursor of the desired 4a-hydroxylated compound **136** through selective epoxidation

dx.doi.org/10.1021/ja506472u | J. Am. Chem. Soc. 2014, 136, 12137−12160

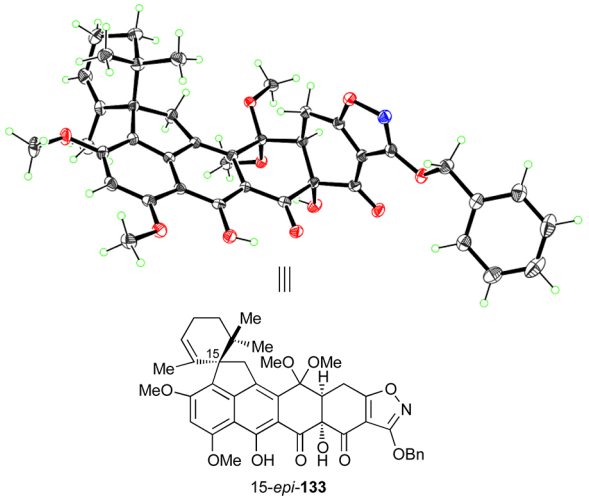

Figure 5. X-ray-derived ORTEP representation of compound 15-*epi*-**133**. Thermal ellipsoids at 30% probability. Gray = carbon, blue = nitrogen, red = oxygen, green = hydrogen.

(to afford **135**) and thence hydrolysis, or through **137** via hydrolysis, enolization, and oxidation, failed. Efforts to generate **134** from **133** employing a variety of conditions, including Lewis acids or protic acids, or under anhydrous conditions (see Supporting Information), however, did not give the desired product but led instead to ketone **137**. Similarly, various conditions to carry out the desired enol ether formation at the quinomethide stage (compound **132**/15-*epi*-**132**) also failed. In addition, a number of transketalization reactions with dimethyl ketal **133** directed at forming an oxa-seleno mixed ketal[67] (intended to be used as a precursor for a selenoxide/syn elimination sequence to produce the desired methylenol ether **134**) ended without success. Attempts to achieve C4a hydroxylation of ketone **137** through enolization followed by oxidation also failed, typically resulting in aromatization to afford **138** (Scheme 23) through β-elimination/tautomerization (see Supporting Information for more details).

We then explored the possibility of achieving C4a hydroxylation using dimethyl ketal **133** (single diastereomer) to generate olefinic compound **141**, whose directed dihydroxylation[68] was expected to yield **142** (see Scheme 24). To this end, exposure of **133** to $NaCNBH_3$ in AcOH produced chromatographically separable methyl ethers **140** (40%) and 5-*epi*-**140** (32%), presumably through reactive oxonium species **139**.[69] The configuration of **140** (and by deduction, of 5-*epi*-**140**) was assigned on the basis of 2D NMR (NOESY) spectroscopic analysis and the observed $^3J_{4a,5}$ = 8.7 Hz coupling constant (see structure **140**, bottom of Scheme 24). Numerous attempts (e.g., Lewis and protic acids) to generate olefin **141** from **140** or 5-*epi*-**140** through elimination of MeOH, however, failed. In several cases, the bis-elimination/tautomerization product **143** was isolated instead. Attempted solvolysis of isomer 5-*epi*-**140** by heating in trifluoroethanol at 70 °C as a means to reach olefin **141** led, surprisingly, to trifluoroethyl ester **144** (70% yield, Scheme 24), presumably through a retro-Dieckmann ring opening reaction.[70]

Unable to reach the $\Delta^{4a,5}$-compound **141** (Scheme 24), we turned to the $\Delta^{4,4a}$-compound **145** as an alternative substrate for the desired C4a hydroxylation. It was envisioned that **145** could be reached from **133** through an oxidative process and then converted to the desired hydroxylated product **147** via

Scheme 24. Attempts To Generate C4a,5-Olefin 141 as a Substrate for Dihydroxylation[a]

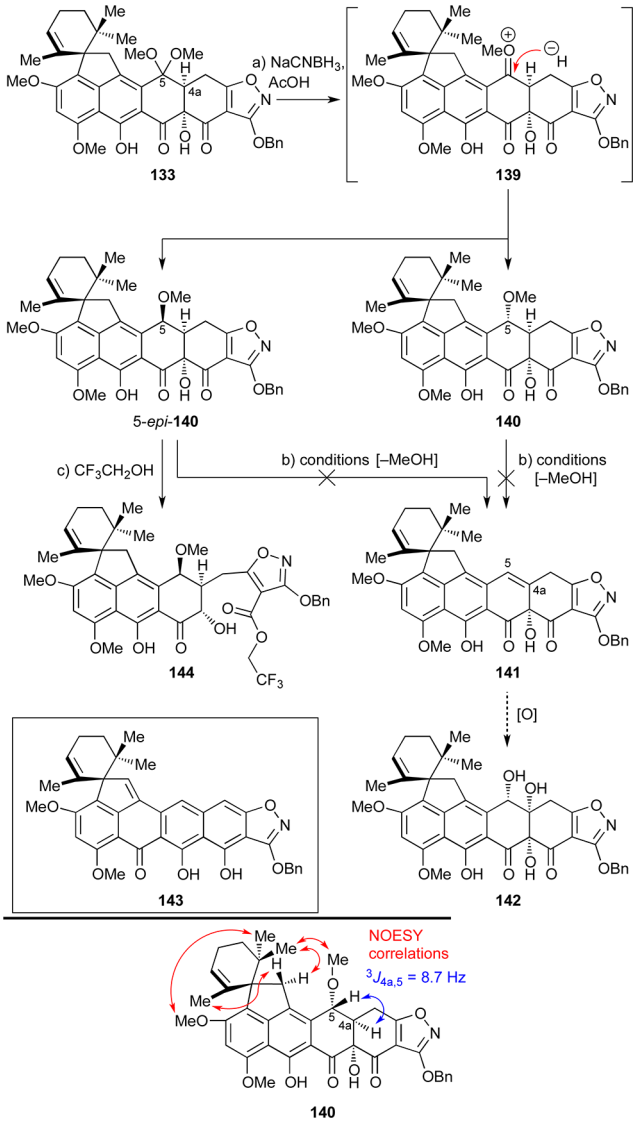

[a]Reagents and conditions: (a) $NaCNBH_3$ (4.3 equiv), AcOH, 25 °C, 40 min, 40% for **140**, 32% for 5-*epi*-**140**, chromatographically separated; (b) various Lewis and Brønsted acids; (c) CF_3CH_2OH, 70 °C, 2 h, 70%.

selective formation and regioselective reductive opening of epoxide **146**, as outlined in Scheme 25. As shown in Scheme 26, execution of this plan began with formation of presumed trianion **148** (KHMDS, −78 °C) followed by quenching with PhSeCl (−78 → −40 °C) to afford phenyl selenide **149** as a single isomer (46% yield + 26% recovered starting material). The configuration of the phenylseleno group within **149** was tentatively assigned on steric grounds (i.e., concavity of the cis-fused AB-ring system). Treatment of selenide **149** with DMDO at −78 °C produced a complex mixture from which seven-membered lactone **152** could be isolated (46% yield), presumably formed through the indicated pathways involving selenoxide **150**, olefin **145**, and either acylketene **151** (pathway A)[71,72] or hydroxy-epoxide **153** (pathway B) (see Scheme 26). Other oxidizing agents (e.g., H_2O_2, *m*-CPBA) led to similar results. In an attempt to shut down the hypothesized hydroxy-epoxide pathway, we prepared TMS ether **154** from **149**

dx.doi.org/10.1021/ja506472u | J. Am. Chem. Soc. 2014, 136, 12137−12160

Scheme 25. Proposed Elaboration of 133 to C4a-Hydroxylated Compound 147 through C4,4a-Olefin 145 and Epoxide 146

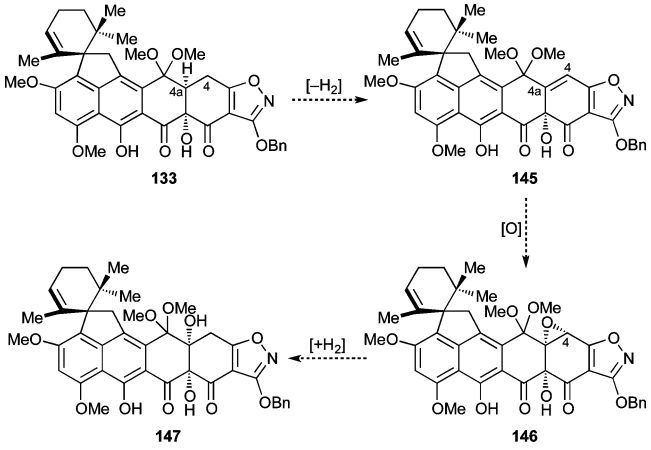

Scheme 26. Attempted Preparation of Olefin 145[a]

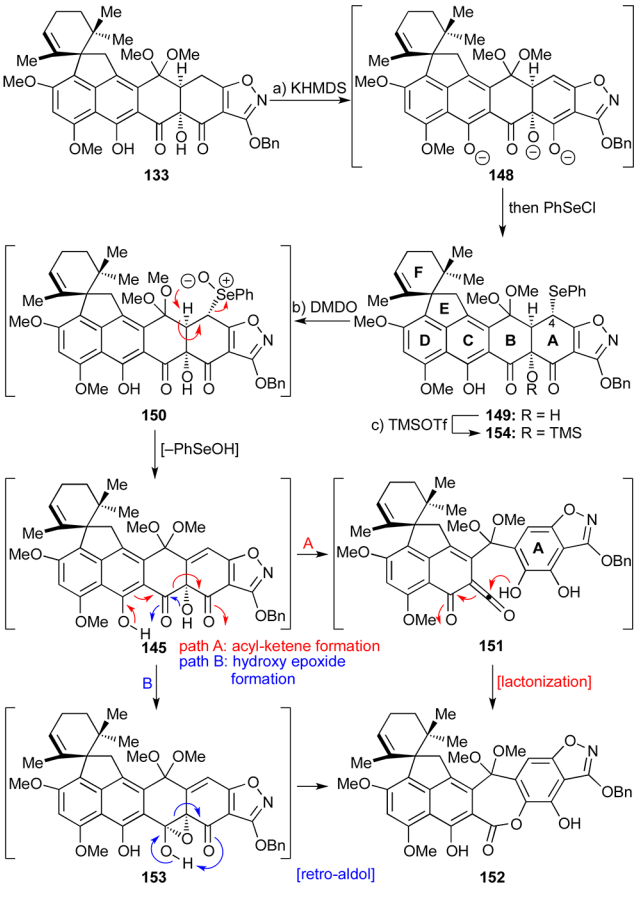

[a]Reagents and conditions: (a) KHMDS (3.3 equiv), THF, −78 °C, 1 h; then PhSeCl (3.5 equiv), −78 → −40 °C, 1 h, 46% (62% brsm) + 26% recovered **133**; (b) from **149**: DMDO (1.0 equiv), THF, −78 °C, 20 min, 46%; from **154**: DMDO (1.5 equiv), THF, −78 °C; then 25 °C, 14 h, 7%; (c) TMSOTf (30 equiv), Et_3N (40 equiv), CH_2Cl_2, 0 °C, 5 min, 62%. OTf = trifluoromethanesulfonate.

(TMSOTf, Et_3N, 62% yield, Scheme 26) and employed it as a substrate in the DMDO oxidation, only to observe the same ring expansion product **152**, albeit in only 7% yield (with concomitant loss of the TMS residue). This outcome seems to tentatively support pathway A, rather than B, for the formation of **152** from **154** (and **149**), although due to the lability of the TMS group the possibility of both pathways operating concurrently cannot be excluded.

A number of other attempts to prepare $\Delta^{4,4a}$-substrates such as **157** (Scheme 27) and **145** (Scheme 28) were made. Thus,

Scheme 27. Attempted Preparation of Enone 157[a]

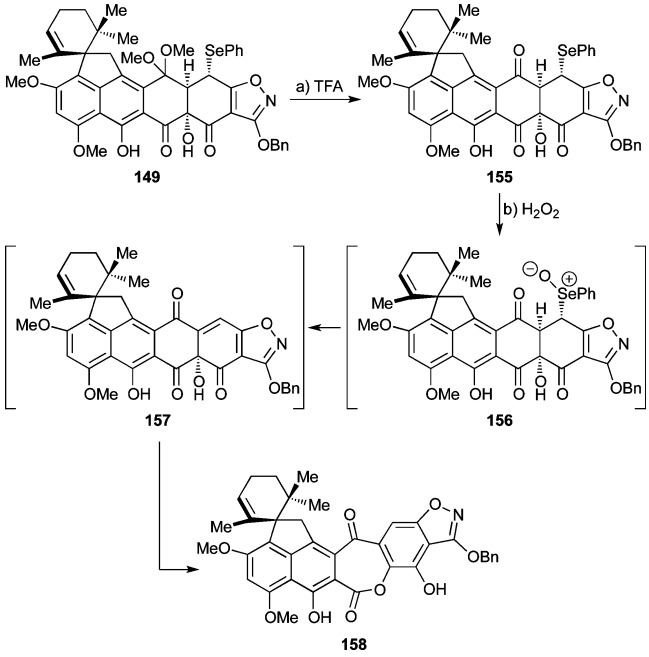

[a]Reagents and conditions: (a) TFA:CH_2Cl_2 (1:2), 0 °C, 40 min, 52%; (b) H_2O_2 (4.5 equiv), CH_2Cl_2, 0 °C, 10 min, 35%.

TFA-induced hydrolysis of ketal **149** gave triketone **155** (52% yield) which was expected to facilitate the formation of **157** through selenoxide formation (**156**) and syn-elimination (see Scheme 27). Unfortunately, however, oxidation of selenide **155** (H_2O_2) did not lead to the expected olefin **157**, but rather to the expanded keto-lactone **158** (35% yield), presumably through selenoxide **156** (see Scheme 27). Similarly, hydroxylation of **133** with Davis oxaziridine through its trianion (KHMDS, −78 °C, 52% yield) followed by ketal hydrolysis (TFA, 63% yield) furnished secondary alcohol **160**, whose attempted dehydration (e.g., through the corresponding mesylate) also failed (see Scheme 28). Iodide **159** (Scheme 28) was also prepared from **133** (KHMDS; NIS, 37%) as a potential precursor to olefinic compound **145**, through oxidation and syn-elimination of the corresponding iodoso compound.[73] Attempts to effect the latter transformation, however, by *m*-CPBA oxidation failed. Moreover, attempted Mukaiyama dehydration[74] from the trianion derived from **133** also did not give the desired olefin **145** (Scheme 28).

Faced with these obstacles toward $\Delta^{4,4a}$-substrates **145** and **157**, we decided to return to $\Delta^{4a,5}$-substrate **141** which we had previously considered but later abandoned (see Scheme 24). Inspired by a report from the Tatsuta group,[75] we reasoned that a 1,3-directed reduction of the C5-carbonyl moiety at the **137** stage could give us access to the C5-hydroxy compound **162**, whose dehydration would lead to the targeted substrate **141** that could serve as a precursor to the desired trihydroxylated intermediate **142** (Scheme 29). However, when **137** was treated with $NaBH(OAc)_3$, we instead isolated the 1,2-directed

dx.doi.org/10.1021/ja506472u | J. Am. Chem. Soc. 2014, 136, 12137−12160

Scheme 28. Other Attempts To Synthesize Olefinic Compounds 141 and 153[a]

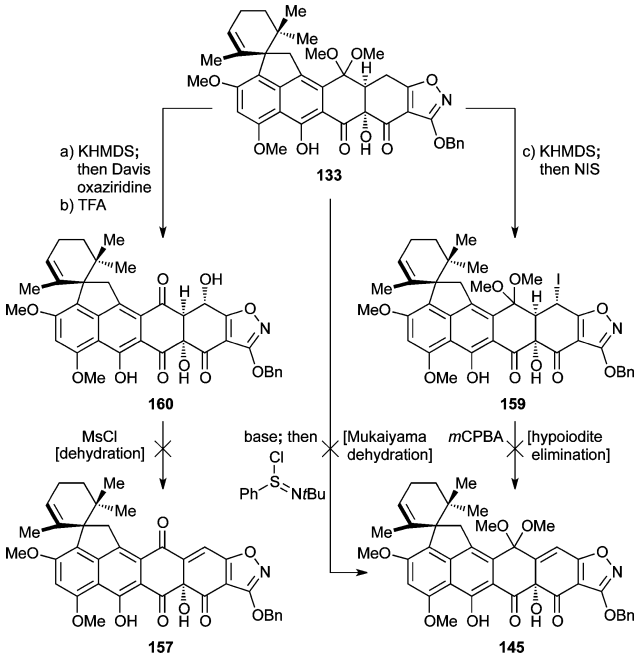

[a]Reagents and conditions: (a) KHMDS (3.8 equiv), THF, −78 °C, 1 h; then Davis oxaziridine (3.5 equiv), −78 → −40 °C, 1 h, 52%; (b) TFA:CH_2Cl_2 (1:3), 0 → 25 °C, 45 min, 63%; (c) KHMDS (3.6 equiv), THF, −78 °C, 80 min; then NIS, −78 → −35 °C, 1 h, 37%. NIS = *N*-iodo-succinimide.

Scheme 29. Attempted Preparation of C5-Hydroxy Compound 162 through 1,3-Directed Reduction and Observation of 1,2-Directed Reduction Product 164[a]

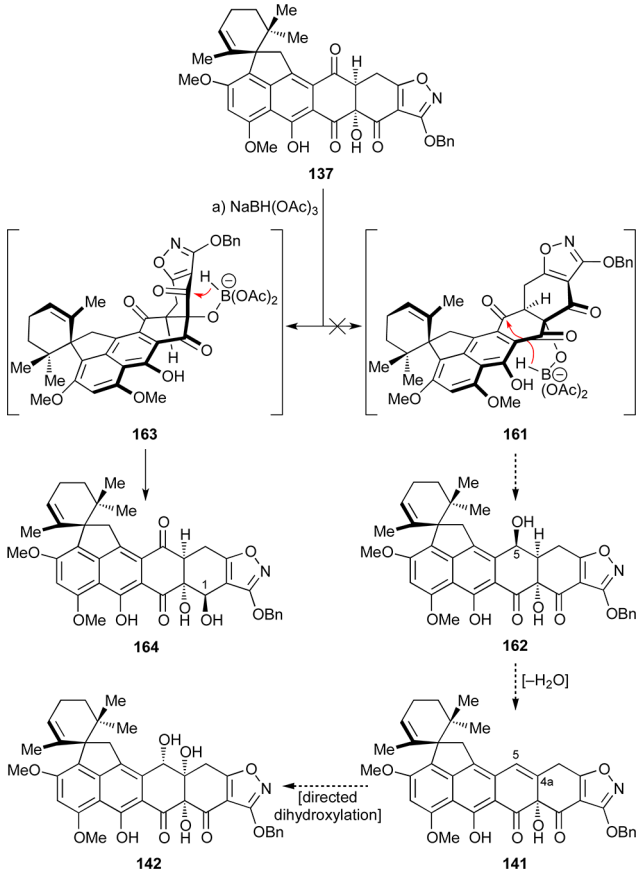

[a]Reagents and conditions: (a) $NaBH(OAc)_3$ (1.3 equiv), EtOH:THF 1:1, 0 → 25 °C, 3.25 h, 35%.

reduction product **164** (35% yield, Scheme 29), along with other unidentifiable products. After further unsuccessful attempts to secure the targeted C5-hydroxy derivative of our heptacyclic compound, we opted to pursue the newly emerged 1,2-directed reduction product **164** as a possible substrate for advancement to viridicatumtoxin B. The rationale behind this choice included the expectation that this intermediate and its derivatives could be resistant to elimination and aromatization side reactions involving rings A and B as previously observed (see Schemes 23 and 24). Brief experimentation led to an improved protocol for the selective reduction of triketone **137** [$NaBH(OAc)_3$, EtOAc:acetone] that delivered alcohol **164** in 53% yield (Scheme 30). The newly generated hydroxy group within the latter compound was protected as a TBS ether through the use of excess TBSOTf (most likely needed due to steric difficulties caused by the concavity of the AB-ring system) to afford compound **165** (64% yield). Conversion of the latter compound to its trianion (**166**) with KHMDS followed by quenching with Davis oxaziridine led to the coveted C4 hydroxylated product **167** in 29% yield (47% based on 39% recovered starting material). Alternative bases (LiHMDS, NaHMDS, or LDA) or equivalents of base did not improve the outcome of this reaction. The configuration of the newly generated C4a hydroxyl moiety within **167** was deduced from NOESY correlations as shown in Scheme 30 (bottom).

In an effort to improve the C4a hydroxylation reaction, we targeted bis-TBS ether **168** (Scheme 31) as a substrate, counting on its dianion to undergo the desired transformation more efficiently. Bis-silylation of **164** with excess TBSOTf required the use of Hünig's base and led to **168** in 57% yield. Interestingly, however, treatment of **168** with KHMDS at −78 °C led rapidly to aromatized product **172** (43% yield), which, in addition to elimination of the OTBS group from its A-ring, had also suffered removal of the TBS group from the phenolic oxygen. These observations suggest that the presumed initially formed dianion **169** is too reactive entering the proposed cascade sequence shown in Scheme 31. Thus, attack of the tertiary alkoxide within **169** on the adjacent carbonyl moiety generates a new alkoxide anion that abstracts the TBS group from the adjacent phenolic position to afford epoxide species **170**. Prompted by the adjacent enolate anion, the epoxide within the latter species undergoes facile *β*-elimination/opening with concomitant loss of the B-ring OTBS group to afford diketone dianion **171**. The generation of the newly established anion at C4 within **171** is facilitated by the isoxazole ring on one side and the quinone moiety on the other. Species **171** then suffers OTBS elimination/ring A aromatization, leading to observed product **172** upon protonation.

Taken together, these extensive investigations on the C4a hydroxylation defined the required structural features for the substrate as (a) protected hydroxyl group at C1 (ring A), (b) free hydroxyl group at C12a (rings A/B), and (c) free phenolic moiety at C11 (ring C). Straying away from any one of these key structural motifs led to either no conversion or rearranged products of undesired structures.

At this point, we decided to move forward and test the remaining steps of the devised synthetic strategy toward viridicatumtoxin B that required reinstallment of the carbonyl

dx.doi.org/10.1021/ja506472u | J. Am. Chem. Soc. 2014, 136, 12137−12160

Scheme 30. Successful C4a Hydroxylation of 164 through Oxidation of Its Trianion[a]

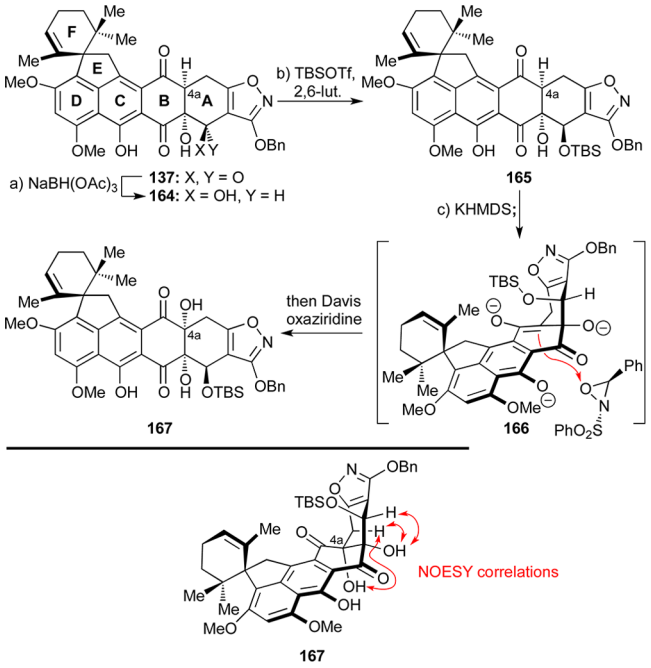

[a]Reagents and conditions: (a) $NaBH(OAc)_3$ (1.2 equiv), EtOAc:acetone 1:1, 40 °C, 3.5 h, 53%; (b) TBSOTf (35 equiv), 2,6-lut. (53 equiv), $ClCH_2CH_2Cl$, 5 → 25 °C, 1.8 h, 64%; (c) KHMDS (3.5 equiv), THF, −78 °C, 65 min; then Davis oxaziridine (4.0 equiv), −78 °C, 40 min, 29% for **167** (47% brsm) + 39% recovered **165**. lut. = lutidine.

Scheme 31. Synthesis and Unsuccessful Attempt To C4a Hydroxylate Bis-TBS Ether 168[a]

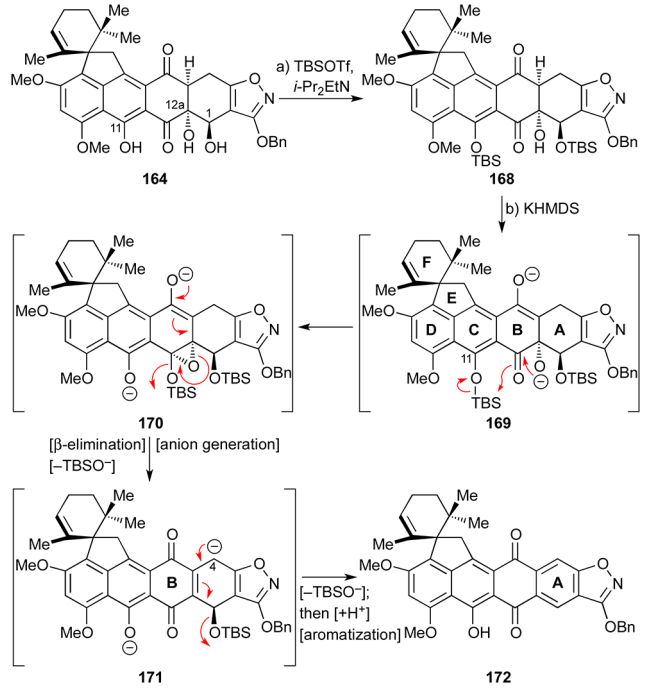

[a]Reagents and conditions: (a) TBSOTf (20 equiv), *i*-Pr_2EtN (30 equiv), CH_2Cl_2, 0 → 25 °C, 33 min, 57%; (b) KHMDS (2.5 equiv), THF, −78 °C, 45 min, 43%.

group at C1, selective removal of the methyl group from the C10 methyl ether, and rupture of the isoxazole moiety to provide the required enol amide functionality at the terminus of the molecule. To this end and as shown in Scheme 32, silyl

Scheme 32. Synthesis of Triketone 136[a]

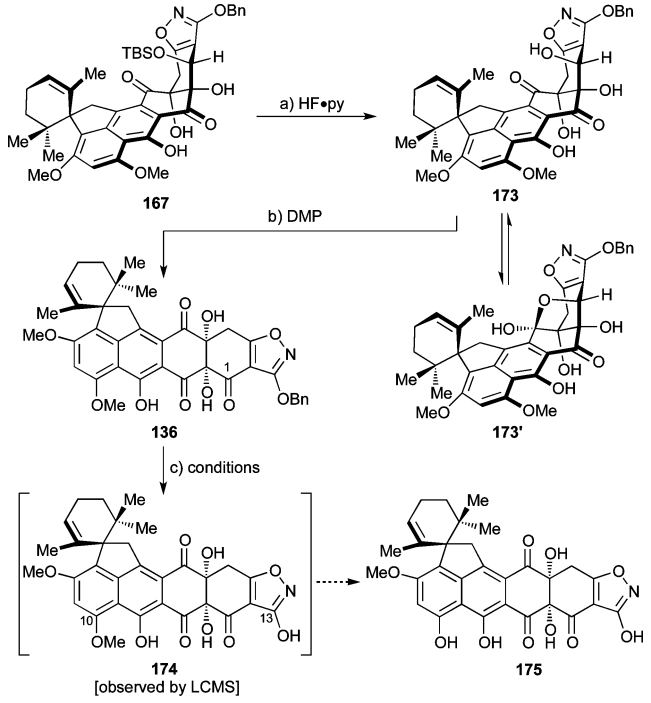

[a]Reagents and conditions: (a) HF·py (excess), MeCN, 0 → 55 °C, 25 h, 66%; (b) DMP (5.2 equiv), $ClCH_2CH_2Cl$, 0 → 40 °C, 4 h, 32%; (c) BCl_3, BBr_3, $AlCl_3$/EtSNa, or 9-I-BBN. DMP = Dess−Martin periodinane, BBN = borabicyclo[3.3.1]nonane.

ether **167** was desilylated (HF·py, 66% yield) to afford C1 hydroxy compound **173** which was assumed to exist in equilibrium with its hemiacetal form **173′** based on its broad ^1H and ^{13}C NMR spectroscopic features. Oxidation of this mixture with DMP resulted in the formation of ketone **136** (32% yield, unoptimized) through reaction of **173**, which apparently drives the equilibrium in the right direction for funneling both isomers (**173** and **173′**) toward the desired product (**136**). The obligatory removal of the methyl group from the C10 phenolic group, however, proved difficult despite the inspiring precedent for such deprotections in the tetracycline series.[19,20b] Thus, attempts to achieve this goal with BCl_3, BBr_3, $AlCl_3$/EtSNa, and 9-I-BBN[76] failed, leading to either decomposition and/or cleavage of the benzyl ether as indicated by LCMS detection of hydroxy-isoxazole **174** (but not **175**).

In contrast to this disappointing result, the rupture of the isoxazole ring planned as the ultimate step of the synthesis proved feasible with substrate **136** under hydrogenation conditions in the presence of Pd black, furnishing 10-*O*-methylviridicatumtoxin B (**176**, 57% yield) as shown in Scheme 33. Interestingly, the spectroscopic data of this compound confirmed its hydroxy-keto form **176** rather than the originally assigned[1] (to viridicatumtoxin B) hydroxy-epoxide structure (i.e., **1′**, Chart 1).

dx.doi.org/10.1021/ja506472u | J. Am. Chem. Soc. 2014, 136, 12137−12160

Scheme 33. Total Synthesis of 10-*O*-Methylviridicatumtoxin B[a]

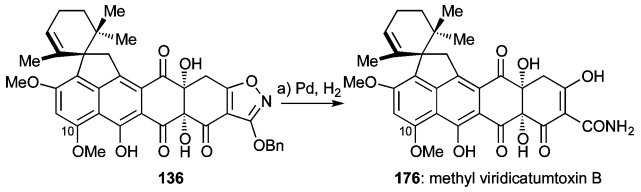

[a]Reagents and conditions: (a) H_2, Pd black (5.3 equiv), MeOH:1,4-dioxane 1:1, 25 °C, 8 min, 57%.

Scheme 34. Final Retrosynthetic Analysis of Viridicatumtoxin B (1)

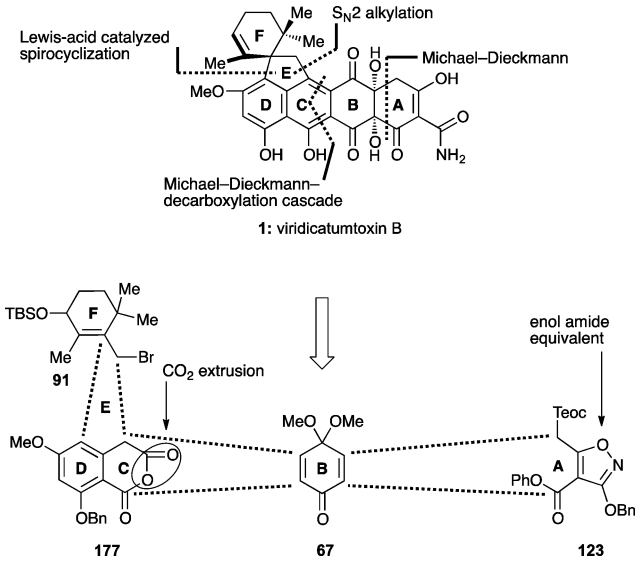

The path-pointing results and intelligence discussed above served as the basis for the final strategy and drive toward viridicatumtoxin B.

Total Synthesis and Structural Revision of Viridicatumtoxin B: Final Drive. Scheme 34 presents the final retrosynthetic analysis and successful strategy that led to the total synthesis of viridicatumtoxin B. Thus, cyclic anhydride **177**, quinone monoketal **67**, allylic bromide **91**, and isoxazole **123** were confidently defined as the required building blocks for the intended route (based on the studies described above). The high modularity of the strategy (i.e., four building blocks of approximately equal sizes) and the accessibility of the starting materials appeared attractive for further development and designed-analogue construction. The adoption of the benzyl ether protecting groups at both the anhydride (**177**) and isoxazole (**123**) fragments offered the advantage of their concurrent removal as the last step in the synthesis. The overall plan called for the union of the anhydride (i.e., **177**) and quinone monoketal (i.e., **67**) fragments through (1) a Michael–Dieckmann/decarboxylation cascade to cast the C ring, (2) an S_N2 alkylation to attach the F ring, (3) a Lewis acid-catalyzed spirocyclization to cast the E ring, and (4) a Michael–Dieckmann sequence to fuse the A-ring as outlined in Scheme 34.

Access to building blocks **67**, **91**, and **123** has already been discussed above, leaving only the preparation of the benzyl-protected anhydride fragment **177** to be described here. Its synthesis and union with the other fragments (**67**, **91**, and **123**) are summarized in Scheme 35. Thus, regioselective demethylation of the known diethyl ester **85** with BBr_3 followed by benzylation (BnBr, Ag_2O) led to benzyl ether **178** in 66% overall yield. Saponification of the ester moieties of the latter (aq NaOH) and heating of the resulting dicarboxylic acid (**179**) with Ac_2O as previously reported[45] furnished desired anhydride **177** in 90% overall yield.

Scheme 35. Synthesis of the Carbon Framework 187 of Viridicatumtoxin B with a C10-OBn Protecting Group[a]

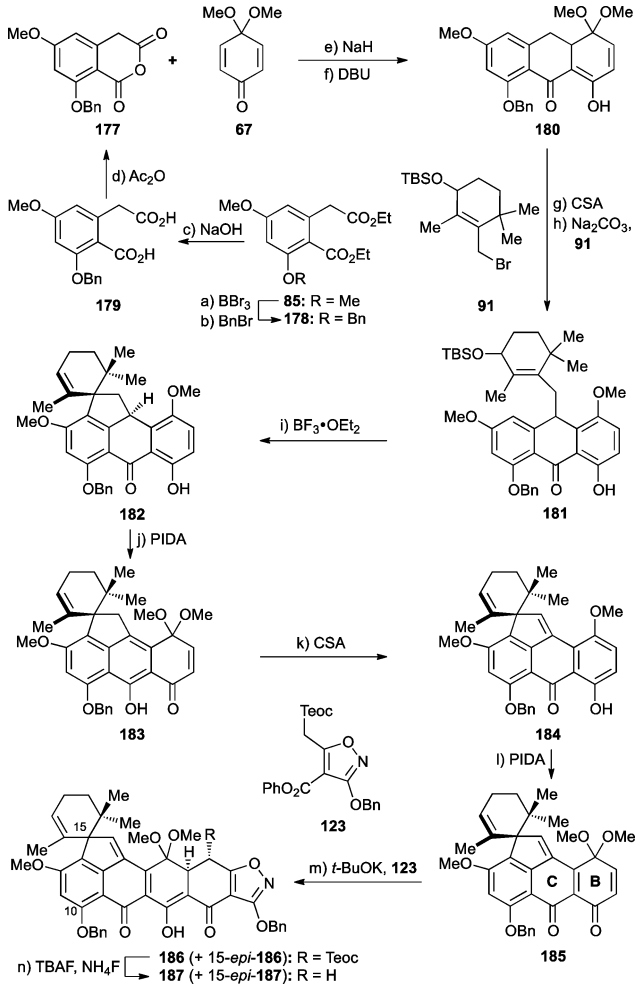

[a]Reagents and conditions: (a) BBr_3 (1.35 equiv), CH_2Cl_2, −78 → 25 °C, 30 min; (b) BnBr (1.1 equiv), Ag_2O (1.9 equiv), DMF, 25 °C, 15 h, 66% for two steps; (c) NaOH (27 equiv), H_2O:EtOH 5:7, reflux, 15 h; (d) Ac_2O (1.1 equiv), toluene, reflux, 1 h, 90% for two steps; (e) **67** (3.0 equiv), NaH (3.0 equiv), THF, 0 °C, 45 min; then 25 °C, 1 h; (f) DBU (5.0 equiv), toluene, 65 °C, 4.5 h, 54% for two steps; (g) CSA (0.02 equiv), CH_2Cl_2, 25 °C, 30 min, 99%; (h) **91** (1.1 equiv), Na_2CO_3 (10 equiv), DMF, 25 °C, 1 h, 77%, ca. 1:1 dr; (i) $BF_3{\cdot}OEt_2$ (0.10 equiv), CH_2Cl_2, 0 °C, 20 min, 73%; (j) PIDA (1.2 equiv), MeOH:CH_2Cl_2 1:1, 0 → 25 °C, 1 h; (k) CSA (0.07 equiv), CH_2Cl_2, 0 °C, 5 min, 85% for two steps; (l) PIDA (1.2 equiv), MeOH:CH_2Cl_2 10:1, 25 °C, 1.5 h, 90%; (m) **123** (1.1 equiv), *t*-BuOK (1.2 equiv), toluene, 25 °C, 15 min, 91%, ca. 2:1 dr; (n) TBAF (10 equiv), NH_4F (20 equiv), degassed THF, 25 °C, 5 min, 86%, ca. 2:1 dr.

Anhydride **177** was reacted with quinone monoketal **67** through the action of NaH (Michael–Dieckmann sequence) followed by treatment of the coupling product with DBU (decarboxylation) to afford tricycle **180** in 54% overall yield.

dx.doi.org/10.1021/ja506472u | J. Am. Chem. Soc. 2014, 136, 12137−12160

Elimination of MeOH from the latter induced by CSA gave the corresponding anthrone (99% yield), which was alkylated with allylic bromide fragment **91** in the presence of Na_2CO_3 to furnish intermediate **181** (77% yield). Exposure of **181** to catalytic amounts of $BF_3{\cdot}OEt_2$ afforded spirocycle **182** in 73% yield. The latter was then treated with PIDA in MeOH:CH_2Cl_2 to give the initially formed quinone monoketal **183** and thence with CSA to afford the phenol *p*-quinomethide **184** (85% yield overall). Phenolic oxidation of the latter with PIDA in MeOH:CH_2Cl_2 then delivered **185** in 90% yield, as observed previously with the corresponding C10-methyl series of substrates (see Scheme 18). Coupling of **185** with isoxazole phenyl ester fragment **123** was effected with *t*-BuOK (Michael reaction/Dieckmann condensation) furnishing heptacyclic compound **186** together with its unseparable C15 epimer (15-*epi*-**186**, ca. 2:1 dr, 91% combined yield). Removal of the now-superfluous Teoc group was accomplished through application of the developed desilylation/decarboxylation procedure (TBAF/NH_4F) to furnish advanced intermediate **187** together with its unseparable isomer 15-*epi*-**187** (ca. 2:1 dr) in 86% combined yield.

The next step in the synthesis entailed hydroxylation of the molecule at C12a (see Scheme 36), a process that was plagued with increased insolubility issues of the benzyl-protected substrate **187**/15-*epi*-**187** as compared to the methyl-protected version employed in the earlier generation route. This necessitated the use of DMDO in the presence of $Ni(acac)_2$ in CH_2Cl_2 (instead of acetone); the efficiency of the reaction remained similar as the previous result after recycling of recovered starting material, yielding C12a-hydroxylated compound **188** together with its 15-epimer (15-*epi*-**188**, 35% yield, 50% yield after one recycle, ca. 2:1 dr, Scheme 36). Employing a solution of DMDO in CH_2Cl_2[77] did not result in a noticeable improvement of conversion or yield, which might be attributed to the decreased stability of DMDO in that solvent. Exposure of the quinomethide mixture (**188** + 15-*epi*-**188**) to $NaCNBH_3$ gave chromatographically separable reduced products **189** (39% yield) and 15-*epi*-**189** (19% yield) whose configurations were assigned by comparisons of their NMR spectroscopic data to those of their corresponding C10-OMe counterparts (as discussed above, the structures of the latter were unambiguously assigned through X-ray crystallographic analysis, see Scheme 23 and Figure 5). Isomer **189** was then advanced to TBS ether **192** as shown in Scheme 36. Thus, treatment of **189** with HCl in aqueous THF led quantitatively to triketone **190**, whose reduction with $NaBH(OAc)_3$ furnished C1-hydroxy compound **191** in 47% yield. The latter was then silylated with TBSOTf in the presence of 2,6-lutidine to afford **192** (61% yield).

The final stretch of the synthesis of viridicatumtoxin B is depicted in Scheme 37. The challenging C4a hydroxylation of

Scheme 36. Synthesis of Enolate-Oxidation Precursor 192[a]

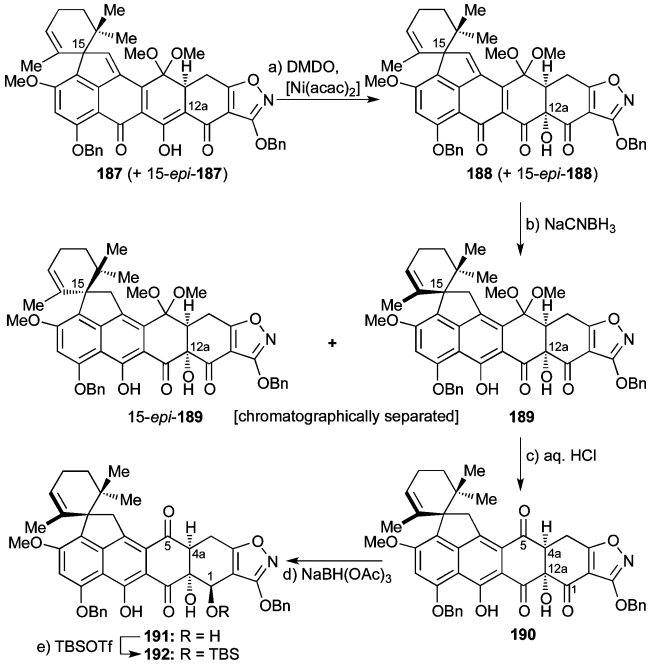

[a]Reagents and conditions: (a) [$Ni(acac)_2$] (0.2 equiv), DMDO (5.1 equiv), CH_2Cl_2, −78 → −60 °C, 6.5 h, 36% (ca. 2:1 dr, 60% brsm), 50% after one recycle; (b) $NaCNBH_3$ (10 equiv), THF, −78 → −60 °C, 90 min, 39% for **189**, 19% for 15-*epi*-**189**, chromatographically separated; (c) 2 N aq. HCl:THF 1:10, 25 °C, 5 h, quant.; (d) $NaBH(OAc)_3$ (1.2 equiv), EtOAc:acetone 1:1, 40 °C, 105 min, 47%; (e) TBSOTf (40 equiv), 2,6-lut. (60 equiv), CH_2Cl_2, 0 → 25 °C, 1 h, 61%.

Scheme 37. Completion of the Total Synthesis of Viridicatumtoxin B (1)[a]

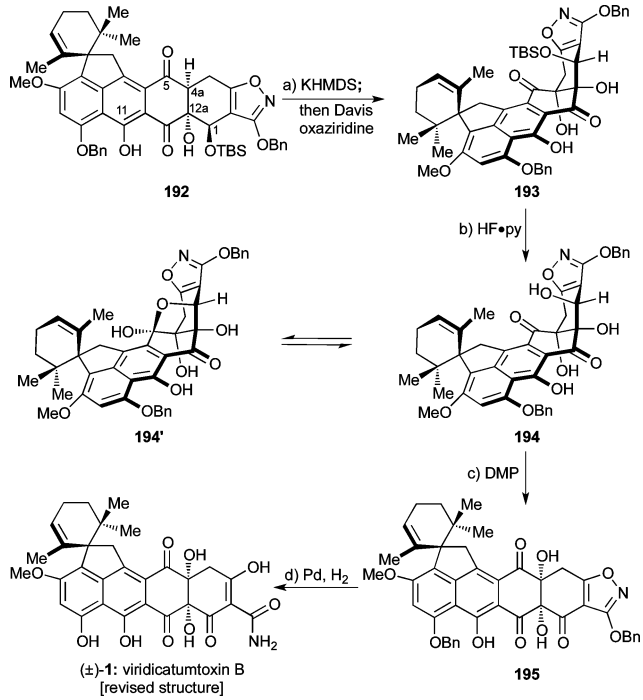

[a]Reagents and conditions: (a) KHMDS (3.4 equiv), THF, −78 °C, 1 h; then Davis ox. (3.9 equiv), −78 °C, 1.7 h, 20% of **193** + 45% recovered **193**; (b) HF·py (excess), MeCN, 0 → 50 °C, 25 h, 61%; (c) DMP (3.0 equiv), $ClCH_2CH_2Cl$, 0 → 50 °C, 7.5 h, 66%; (d) H_2, Pd black (4.9 equiv), 1,4-dioxane:MeOH 1:1, 25 °C, 8 min, 98%.

precursor **192** proceeded in the presence of KHMDS (added first at −78 °C to form the presumed trianion of **192**) and Davis oxaziridine (added thence at −78 °C) to afford hydroxylated product **193** (20% yield + 45% recovered starting material). Desilylation of **193** with HF·py furnished polyhydroxy compound **194**, whose equilibrium with its lactol form (**194**′) was evident from the ^1H NMR spectra ($CDCl_3$, 500

dx.doi.org/10.1021/ja506472u | J. Am. Chem. Soc. 2014, 136, 12137−12160

MHz) at ambient temperature (broad signals) and −40 °C (two sets of sharp signals, ca. 2:1 ratio). (This was the same phenomenon we encountered with their 10-methoxy counterparts **173**/**173′**, Scheme 32, as discussed above). Oxidation of the so-obtained mixture (**194** + **194′**) with DMP then gave triketone **195** in 66% yield, with the lactol form **194′** being funneled into the oxidation pathway by the equilibrium. Pleasantly, hydrogenation of the latter compound (Pd black, H_2) produced synthetic viridicatumtoxin B (**1**) in 98% yield through cleavage of the two benzyl ethers, rupture of the isoxazole N−O bond, and tautomerization of the resulting hydroxy-imine to the desired primary amide.

The physical properties of synthetic viridicatumtoxin B were consistent with those of the authentic natural product and our proposed structure (**1**). The ^{1}H NMR data of synthetic viridicatumtoxin B (**1**) were in good agreement with those reported in the literature.[1] However, we observed a ^{13}C NMR signal at δ = 194.1 ppm for C5, whereas the reported chemical shift for the proposed C5 epoxy-hemiacetal in the originally assigned structure was δ = 116.4 ppm. Therefore, a detailed re-examination of the authentic carbon NMR spectrum (obtained from Professor W. G. Kim) of natural viridicatumtoxin B was conducted. Indeed, the signal near δ = 194 ppm was observable in the authentic spectrum of the natural product. We assume that, due in part to the minute amounts of this complex natural product isolated, an erroneous interpretation of the HMBC spectrum seemingly supported the original structural assignment (see the Supporting Information for more details and copies of the authentic spectra). We therefore revised the originally proposed structure of viridicatumtoxin B (**1′**)[1] to that shown in Scheme 37 (i.e., **1**). Furthermore, our synthetic material crystallized from CH_2Cl_2/EtOH in suitable form for X-ray crystallographic analysis [mp = 245−247 °C (decomp)] and proved unambiguously its structure as shown in **1** (see ORTEP representation, Figure 6).[55]

Biological Evaluation of Synthetic (±)-Viridicatumtoxin B and Analogues. Employing the developed synthetic technologies in this research program, we were able to access not only (±)-viridicatumtoxin B [(±)-**1**] but also a number of analogues that are simpler and easier to synthesize for biological evaluation (see Chart 3 for structures). Specifically, analogues

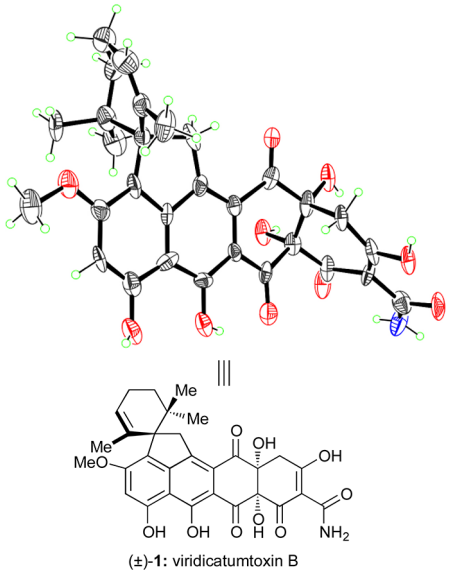

Figure 6. X-ray-derived ORTEP representation of synthetic viridicatumtoxin B (**1**). Thermal ellipsoids at 30% probability. Gray = carbon, blue = nitrogen, red = oxygen, green = hydrogen.

Chart 3. Molecular Structures of Natural Viridicatumtoxin A (2), Synthetic Viridicatumtoxin B (1), Synthesized Viridicatumtoxin Analogues (V2−V6), and Tetracycline Drugs Minocycline (7) and Tigecycline (9)

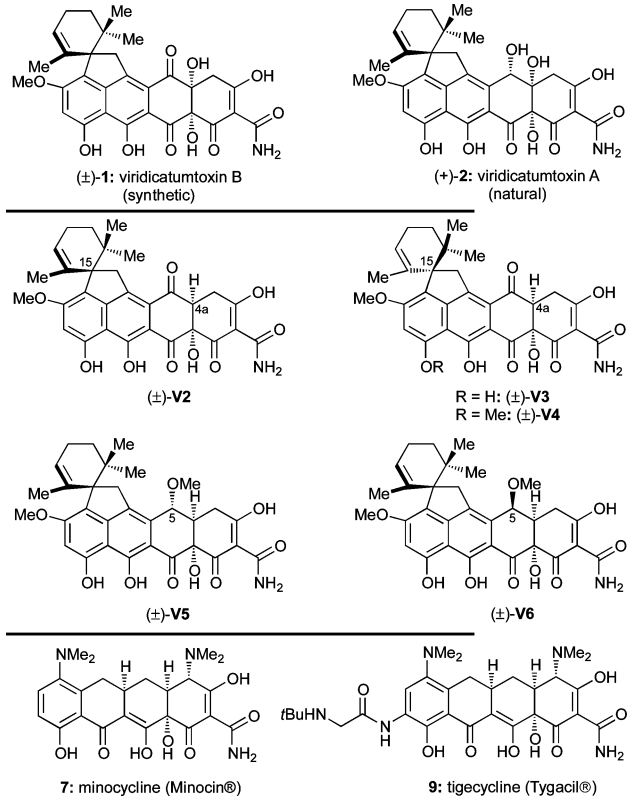

(±)-**V2**, (±)-**V3**, (±)-**V4**, (±)-**V5**, and (±)-**V6**, all lacking the C4a hydroxyl group so cumbersome to install, were synthesized (see Supporting Information for their synthesis) and, together with (±)-**1**, were tested against a number of bacterial strains and compared to natural viridicatumtoxin B [(+)-**1**, reported values[1]], natural viridicatumtoxin A [(+)-**2**, obtained from Professor Yi Tang], minocycline (Minocin, **7**), and tigecycline (Tygacil, **9**) (see Chart 3 for structures).

As shown in Table 1, all of the viridicatumtoxins and analogues tested exhibited antibacterial efficacy against Gram-positive bacteria [(*E. faecalis S613, E. faecium 501,* and methicillin-resistant *Staphylococcus aureus 371* (MRSA 371)] but were largely inactive against Gram-negative bacteria (i.e., *A. baumannii AB210*). Thus, synthetic viridicatumtoxin B [(±)-**1**] exhibited comparable antibacterial properties against these strains (*E. faecalis S613*, *E. faecium 501*, and MRSA 371: MIC = 1, 0.5, and 4 μg/mL, respectively) to those reported for natural viridicatumtoxin B [(+)-**1**] against similar strains (*E. faecalis* KCTC5191, *E. faecium* KCTC3122, MRSA CCARM3167: MIC = 2, 0.5, and 0.5 μg/mL, respectively), despite the racemic nature of the former. The potencies of synthetic (±)-**1** were also comparable to those reported[1] for natural viridicatumtoxin A [(+)-**2**] against similar strains (see Table 1).

Viridicatumtoxin analogue (±)-**V2**, lacking the C4a hydroxyl group, displayed high potency against the same strains (*E. faecalis S613*: MIC = 0.5 μg/mL; *E. faecium 501*: MIC = 0.5 μg/

dx.doi.org/10.1021/ja506472u | J. Am. Chem. Soc. 2014, 136, 12137−12160

Table 1. Minimum Inhibitory Concentration (MIC) Data of Compounds against Gram-Positive and Gram-Negative Bacteria and Comparison with Selected Literature Data

	Gram-(+)						Gram-(−)		
	this study[a]			ref 1			this study[a]	ref 1	
entry	*E. faecalis* S613	*E. faecium* 501	*MRSA* 371	*E. faecalis* KCTC5191[b]	*E. faecium* KCTC3122[b]	*MRSA* CCARM3167[b]	*A. baumannii* AB210	*A. calcoaceticus* KCTC2357[b]	*E. coli* CCARM1356[b]
(−)-**7**	4	4	2	–	–	–	4	–	–
(−)-**9**	0.5	0.5	1	–	–	–	0.5	–	–
(±)-**1**	1	0.5	4	2[c]	0.5[c]	0.5[c]	64	1[c]	>64[c]
(+)-**2**[78]	1	1	4	4	1	0.25	64	2	>64
(±)-**V2**	0.5	0.5	2	–	–	–	64	–	–
(±)-**V3**	4	2	8	–	–	–	64	–	–
(±)-**V4**	4	4	4	–	–	–	64	–	–
(±)-**V5**	1	1	8	–	–	–	64	–	–
(±)-**V6**	0.5	0.5	2	–	–	–	64	–	–

[a]MIC assays were run in triplicate; data are given in units of μg/mL. [b]Taken from ref 1 for comparison. [c]Enantiopure material [(+)-**1**] isolated from *Penicillium* sp. FR11 was used in ref 1.

mL; MRSA 371: MIC = 2 μg/mL) leading to the conclusion that this functionality is not necessary for antibacterial activity in this subclass of tetracyclines. Of note is the loss of considerable potency in going from the natural to the opposite C15 configuration [analogues (±)-**V3** and (±)-**V4**] as shown in Table 1. Interestingly, methyl ethers (±)-**V5** and (±)-**V6**, also lacking the C4a hydroxyl moiety, demonstrated potent antibacterial properties against *E. faecalis S613* [(±)-**V5**: MIC = 1 μg/mL; (±)-**V6**: MIC = 0.5 μg/mL], *E. faecium 501* [(±)-**V5**: MIC = 1 μg/mL; (±)-**V6**: MIC = 0.5 μg/mL], and MRSA 371 [(±)-**V5**: MIC = 8 μg/mL; (±)-**V6**: MIC = 2 μg/mL]. These results further support the conclusion that the C4a hydroxyl group of the viridicatumtoxin analogues is not necessary for biological activity (see Table 1). Finally, despite the previously reported activity of viridicatumtoxins against several Gram-negative bacterial strains,[1] our tested compounds were inactive against *A. baumannii AB210*, consistent with previous reports suggesting that the C4-dimethylamino residue is important for imparting the broad-spectrum activity observed for both minocycline (**7**) and tigecycline (**9**).[79] Incorporation of such a moiety into the viridicatumtoxin scaffold could expand their antibacterial profile as well as improve their pharmacological properties.[79]

In preliminary experiments to probe the mode-of-action of viridicatumtoxin analogues, time-kill assays were performed to measure the killing of *E. faecalis S613* by viridicatumtoxin A (**2**) and (±)-**V6** alongside tigecycline (**9**). The motivation for this study was previous reports that tetracycline analogues with an aromatic C-ring [e.g., viridicatumtoxin A (**2**) and (±)-**V6**] act via a bactericidal mechanism as opposed to a bacteriostatic one (i.e., inhibition of the bacterial ribosome).[80] Our time-kill assays clearly indicated that both viridicatumtoxin A (**2**) and (±)-**V6** act bacteriostatically and not bactericidally (see Supporting Information for additional data).[81] Although (±)-**V6** did not meet the criterion for bactericidal activity, the ability of (±)-**V6** to kill *E. faecalis S613* was similar to the clinically used and bacteriostatic antibiotic tigecycline (**9**). If viridicatumtoxins [i.e., viridicatumtoxin A (**2**) and (±)-**V6**] are indeed inhibitors of the bacterial ribosome, as opposed to inhibitors of UPP synthase as suggested by Tomoda and co-workers,[3] then based on the structure of tigecycline (**9**) bound to the *Thermus thermophilus* ribosome, the C4−C7 positions of viridicatumtoxins are likely ideal sites for further modifications, as those positions do not directly interact with the ribosome.[82]

CONCLUSIONS

In summary, we described herein the evolution of synthetic strategies toward viridicatumtoxin B [(±)-**1**] that finally led to the development of a viable route for the total synthesis of this intriguing natural product. During the course of our studies, we discovered various chemical transformations and acquired synthetic knowledge expected to prove valuable for the synthesis of other fungal tetracyclines and related compounds. In particular, we delineated tactics and strategic requirements for the installation of the hydroxyl groups at C4a and C12a. Other important findings include the anthrone alkylation/spirocyclization reactions to create the congested EF-spirosystem as well as the Michael−Dieckmann cascade reactions that led to the construction of rings A and C. Most notably, our synthetic efforts led to structural revision and configurational assignment of viridicatumtoxin B. Furthermore, application of the developed synthetic technologies allowed the preparation of a number of simpler analogues of the natural product endowed with antibacterial properties comparable with those of viridicatumtoxins A and B, despite their racemic nature. The described chemistry paves the way for further studies, including an asymmetric synthesis of viridicatumtoxins and the design, synthesis, and biological evaluation of other analogues for potential applications as antibacterial agents.[83]

ASSOCIATED CONTENT

Supporting Information

Experimental procedures and characterization data for key compounds (pdf and cif files). This material is available free of charge via the Internet at http://pubs.acs.org.

AUTHOR INFORMATION

Corresponding Author

kcn@rice.edu

Present Address

[#]Department of Chemistry, Rice University, 6100 Main St., Houston, Texas 77005.

Author Contributions

The manuscript was written through contributions of all authors. All authors have given approval to the final version of the manuscript.

Author Contributions

[⊥]These authors contributed equally.

Notes

The authors declare no competing financial interest.

■ ACKNOWLEDGMENTS

We thank Drs. D. H. Huang and L. Pasternack for NMR spectroscopic, Drs. G. Siuzdak and C. Pennington for mass spectrometric, and Drs. R. K. Chadha and C. Moore for X-ray crystallographic assistance. We thank Prof. W.-G. Kim for graciously providing scanned NMR spectra of natural viridicatumtoxin B. We additionally thank Prof. Yi Tang (UCLA) for generously providing a sample of natural viridicatumtoxin A. K.C.N. acknowledges financial support from the National Institutes of Health (USA) (grant AI055475), the Skaggs Institute of Research, the Cancer Prevention & Research Institute of Texas (CPRIT), and The Welch Foundation. Fellowships to C.R.H.H. (NSF Graduate Research Fellowship), C.N. (Feodor Lynen Research Fellowship, Alexander von Humboldt Foundation), H.A.I. (Marie-Curie International Outgoing Fellowship, European Commission), and A.E. (Fundación Alfonso Martín Escudero) are gratefully appreciated. Y.S. acknowledges financial support from the National Institutes of Health (USA) (grant AI080714).

■ REFERENCES

(1) Zheng, C. J.; Yu, H. E.; Kim, E. H.; Kim, W. G. *J. Antibiot.* **2008**, *61*, 633−637.
(2) Hutchison, R. D.; Steyn, P. S.; van Rensberg, S. J. *Toxicol. Appl. Pharmacol.* **1973**, *24*, 507−509.
(3) Inokoshi, J.; Nakamura, Y.; Hongbin, Z.; Uchida, R.; Nonaka, K.; Masuma, R.; Tomoda, H. *J. Antibiot.* **2013**, *66*, 37−41.
(4) Duggar, B. M. *Ann. N.Y. Acad. Sci.* **1948**, *51*, 177−181.
(5) Dougherty, T. J.; Pucci, M. J. *Antibiotic Discovery and Development*; Springer: New York, 2012.
(6) Tally, F. T.; Ellestad, G. A.; Testa, R. T. *J. Antimicrob. Chemother.* **1995**, *35*, 449−452.
(7) Sutcliffe, J. A.; O'Brien, W.; Fyfe, C.; Grossman, T. H. *Antimicrob. Agents Chemother.* **2013**, *57*, 5548−5558.
(8) Chopra, I.; Roberts, M. *Microbiol. Mol. Biol. R.* **2001**, *65*, 232−260.
(9) Breinholt, J.; Jensen, G. W.; Kjaer, A.; Olsen, C. E.; Rosendahl, C. N. *Acta Chem. Scand.* **1997**, *51*, 855−860.
(10) Wong, S. M.; Kullnig, R.; Dedinas, J.; Appell, K. C.; Kydd, G. C.; Gillum, A. M.; Cooper, R.; Moore, R. *J. Antibiot.* **1993**, *46*, 214−221.
(11) Ishimaru, T.; Tsuboya, S.; Saijo, T. (Takeda Chem. Ind. Ltd.). JP Patent 06,40995A, March 17, 1993.
(12) (a) Kodukula, K.; Arcuri, M.; Cutrone, J. Q.; Hugill, R. M.; Lowe, S. E.; Pirnik, D. M.; Shu, Y. Z.; Fernandes, P. B.; Seethala, R. *J. Antibiot.* **1995**, *48*, 1055−1059. (b) Shu, Y. Z.; Cutrone, J. F. Q.; Klohr, S. E.; Huang, S. *J. Antibiot.* **1995**, *48*, 1060−1065.
(13) (a) Conover, L. H.; Korst, J. J.; Butler, K.; Woodward, R. B.; Johnston, J. D. *J. Am. Chem. Soc.* **1962**, *84*, 3222−3224. (b) Korst, J. J.; Johnston, J. D.; Butler, K.; Bianco, E. J.; Conover, L. H.; Woodward, R. B. *J. Am. Chem. Soc.* **1968**, *90*, 439−457.
(14) Gurevich, A. I.; Karapetyan, M. G.; Kolosov, M. N.; Korobko, V. G.; Onoprienko, V. V.; Popravko, S. A.; Shemyakin, M. M. *Tetrahedron Lett.* **1967**, 131−134.
(15) (a) Muxfeldt, H.; Hardtman, G.; Kathawal, F.; Vedejs, E.; Mooberry, J. B. *J. Am. Chem. Soc.* **1968**, *90*, 6534−6536. (b) Muxfeldt, H.; Haas, G.; Hardtmann, G.; Kathawala, F.; Mooberry, J. B.; Vedejs, E. *J. Am. Chem. Soc.* **1979**, *101*, 689−701.
(16) For a review, see: (a) Barton, D. H. R. *Pure Appl. Chem.* **1971**, *25*, 5−23. Barton et al. published a series of "back to back" papers on their work, starting with: (b) Barton, D. H. R.; Magnus, P. D. *J. Chem. Soc. C* **1971**, 2164−2166.
(17) Wasserman, H. H.; Lu, T. J.; Scott, A. I. *J. Am. Chem. Soc.* **1986**, *108*, 4237−4238.
(18) (a) Stork, G.; Hagedorn, A. A. *J. Am. Chem. Soc.* **1978**, *100*, 3609−3611. (b) Stork, G.; Yee, Y. K. *Can. J. Chem.* **1984**, *62*, 2627−2628. (c) Stork, G.; LaClair, J. J.; Spargo, P.; Nargund, R. P.; Totah, N. *J. Am. Chem. Soc.* **1996**, *118*, 5304−5305.
(19) Tatsuta, K.; Yoshimoto, T.; Gunji, H.; Okado, Y.; Takahashi, M. *Chem. Lett.* **2000**, 646−647.
(20) (a) Charest, M. G.; Siegel, D. R.; Myers, A. G. *J. Am. Chem. Soc.* **2005**, *127*, 8292−8293. (b) Charest, M. G.; Lerner, C. D.; Brubaker, J. D.; Siegel, D. R.; Myers, A. G. *Science* **2005**, *308*, 395−398. (c) Brubaker, J. D.; Myers, A. G. *Org. Lett.* **2007**, *9*, 3523−3525. (d) Sun, C. X.; Wang, Q.; Brubaker, J. D.; Wright, P. M.; Lerner, C. D.; Noson, K.; Charest, M. G.; Siegel, D. R.; Wang, Y. M.; Myers, A. G. *J. Am. Chem. Soc.* **2008**, *130*, 17913−17927. (e) Kummer, D. A.; Li, D. R.; Dion, A.; Myers, A. G. *Chem. Sci.* **2011**, *2*, 1710−1718. (f) Wright, P. M.; Myers, A. G. *Tetrahedron* **2011**, *67*, 9853−9869.
(21) Wzorek, J. S.; Knopfel, T. F.; Sapountzis, I.; Evans, D. A. *Org. Lett.* **2012**, *14*, 5840−5843.
(22) (a) Kabuto, C.; Silverton, J. V.; Akiyama, T.; Sankawa, U.; Hutchison, R. D.; Steyn, P. S.; Vleggaar, R. *J. Chem. Soc., Chem. Commun.* **1976**, 728−729. (b) Silverton, J. V.; Kabuto, C.; Akiyama, T. *Acta Crystallogr., Sect. B: Struct. Crystallogr. Cryst. Chem.* **1982**, *38*, 3032−3037.
(23) (a) De Jesus, A. E.; Hull, W. E.; Steyn, P. S.; Van Heerden, F. R.; Vleggaar, R. *J. Chem. Soc., Chem. Commun.* **1982**, 902−904. (b) Horak, R. M.; Maharaj, V. J.; Marais, S. F.; Van Heerden, F. R.; Vleggaar, R. *J. Chem. Soc., Chem. Commun.* **1988**, 1562−1564.
(24) Chooi, Y. H.; Cacho, R.; Tang, Y. *Chem. Biol.* **2010**, *17*, 483−494.
(25) Chooi, Y. H.; Wang, P.; Fang, J. X.; Li, Y.; Wu, K.; Wang, P.; Tang, Y. *J. Am. Chem. Soc.* **2012**, *134*, 9428−9437.
(26) Chooi, Y. H.; Hong, Y. J.; Cacho, R. A.; Tantillo, D. J.; Tang, Y. *J. Am. Chem. Soc.* **2013**, *135*, 16805−16808.
(27) Koyama, N.; Inokoshi, J.; Tomoda, H. *Molecules* **2013**, *18*, 204−224.
(28) Nicolaou, K. C.; Nilewski, C.; Hale, C. R. H.; Ioannidou, H. A.; ElMarrouni, A.; Koch, L. G. *Angew. Chem., Int. Ed.* **2013**, *52*, 8736−8741.
(29) (a) Dufraisse, C.; Rigaudy, J.; Basselier, J.-J.; Cuong, N. K. *C. R. Acad. Sci.* **1965**, *260*, 5031−5036. (b) Rigaudy, J. *Pure Appl. Chem.* **1968**, *16*, 169−186. (c) Rigaudy, J.; Deletang, C.; Basselier, J.-J. *C. R. Acad. Sci. Paris* **1969**, *268*, 344−347. (d) Rigaudy, J.; Sparfel, D. *Bull. Chem. Soc. Fr.* **1972**, 3441−3446. (e) Rigaudy, J.; Sparfel, D. *Tetrahedron* **1978**, *34*, 113−121. (f) Sparfel, D.; Gobert, F.; Rigaudy, J. *Tetrahedron* **1980**, *36*, 2225−2235. (g) Santamaria, J.; Rigaudy, J. *Tetrahedron* **1980**, *36*, 2453−2457. (h) Rigaudy, J.; Scribe, P.; Brelière, C. *Tetrahedron* **1981**, *37*, 2585−2593. (i) Rigaudy, J.; Caspar, A.; Lachgar, M.; Maurette, D.; Chassagnard, C. *Bull. Chem. Soc. Fr.* **1992**, *129*, 16−24. (j) Rigaudy, J.; Lachgar, M.; Saad, M. M. A. *Bull. Chem. Soc. Fr.* **1994**, *131*, 177−187. (k) Rigaudy, J.; Lachgar, M.; Caspar, A.; Chassagnard, C. *Bull. Chem. Soc. Fr.* **1996**, *133*, 481−490. (l) Rigaudy, J.; Lachgar, M. *Tetrahedron Lett.* **1997**, *38*, 2267−2270.
(30) For cobalt-mediated endoperoxide rearrangements, see: Boyd, J. D.; Foote, C. S.; Imagawa, D. K. *J. Am. Chem. Soc.* **1980**, *102*, 3641−3642.
(31) Other iron species are capable of inducing these rearrangements, see: Kamata, M.; Satoh, C.; Kim, H.-S.; Wataya, Y. *Tetrahedron Lett.* **2002**, *43*, 8313−8317.
(32) For reviews on endoperoxide rearrangements, see: (a) Waldemar, A.; Balci, M. *Tetrahedron* **1980**, *36*, 833−858. (b) Balci, M. *Chem. Rev.* **1981**, *81*, 90−108.
(33) Kadás, I.; Árvai, G.; Horváth, G. *Org. Prep. Proced.* **1998**, *30*, 79−85.
(34) Tietze, L. F.; Singidi, R. R.; Gericke, K. M. *Chem.—Eur. J.* **2007**, *13*, 9939−9947.
(35) Savard, J.; Brassard, P. *Tetrahedron* **1984**, *40*, 3455−3464.
(36) For selected examples, see ref 34 and Grunwell, J. R.; Karipides, A.; Wigal, C. T.; Heinzman, S. W.; Parlow, J.; Surso, J. A.; Clayton, L.; Fleitz, F. J.; Daffner, M.; Stevens, J. E. *J. Org. Chem.* **1991**, *56*, 91−95.

(37) Cameron, D. W.; Raverty, W. D. *Aust. J. Chem.* **1976**, *29*, 1523−1533.
(38) (a) Schaltegger, A.; Steiger, W. *Arch. Pharm.* **1986**, *319*, 575−576. (b) Müller, K.; Gürster, D.; Piwek, S.; Wiegrebe, W. *J. Med. Chem.* **1993**, *36*, 4099−4107.
(39) Thoma, K.; Holzmann, C. *Eur. J. Pharm. Biopharm.* **1998**, *46*, 201−208.
(40) (a) Stoll, A.; Becker, B.; Helfenstein, A. *Helv. Chem. Acta.* **1950**, *33*, 313−316. (b) Geiger, K. *Chem. Ber.* **1974**, *107*, 2976−2984. See also: (c) Müller, K.; Eibler, E.; Mayer, K. K.; Wiegrebe, W.; Klug, G. *Arch. Pharm.* **1986**, *319*, 2−9. (d) Yamaguchi, M.; Hasebe, K.; Uchida, M.; Higashi, H.; Minami, T. *Bull. Chem. Soc. Jpn.* **1989**, *62*, 2745−2747. (e) Kuhnert, N.; Molod, H. Y. *Tetrahedron Lett.* **2005**, *46*, 7571−7573.
(41) (a) Davis, B. R.; Hinds, M. G.; Johnson, S. J. *Aust. J. Chem.* **1985**, *38*, 1815−1825. (b) Namba, K.; Yamamoto, H.; Sasaki, I.; Mori, K.; Imagawa, H.; Mugio, N. *Org. Lett.* **2008**, *10*, 1767−1770. (c) Yadav, J. S.; Thirupathaiah, B.; Al Khazim AlGhamdi, A. *Eur. J. Org. Chem.* **2012**, 2072−2076. (d) Wang, J.; Zhang, L.; Jing, Y.; Huang, W.; Zhou, X. *Tetrahedron Lett.* **2009**, *50*, 4978−4982. See also: (e) Pittman, C. U., Jr.; Miller, W. G. *J. Am. Chem. Soc.* **1973**, *95*, 2947−2956. (f) Miller, W. G.; Pittman, C. U., Jr. *J. Org. Chem.* **1974**, *39*, 1955−1956. (g) Gassman, P. G.; Ray, J. A.; Wenthold, P. G.; Mickelson, J. W. *J. Org. Chem.* **1991**, *56*, 5143−5146.
(42) (a) Ma, S.; Zhang, J. *Tetrahedron* **2003**, *59*, 6273−6282. (b) Werle, S.; Fey, T.; Neudörfl, J. M.; Schmalz, H.-G. *Org. Lett.* **2007**, *9*, 3555−3558. (c) Liu, H.; Wang, Y.-H.; Zhu, L.-L.; Li, X.-X.; Zhou, W.; Chen, Z.; Hu, W.-X. *Tetrahedron Lett.* **2011**, *52*, 2990−2993.
(43) Moriarty, R. M.; Prakash, O. *Org. React.* **2004**, 327−415.
(44) (a) Meyer, K. H. *Justus Liebigs Ann. Chem.* **1911**, *379*, 37−78. (b) Thomson, R. H. *Q. Rev. Chem. Soc.* **1956**, *10*, 27−43. (c) Kündig, E. P.; Enríquez García, A.; Lomberget, T.; Bernardinelli, G. *Angew. Chem., Int. Ed.* **2006**, *45*, 98−101. (d) Reviriego, F.; Alkorta, I.; Elguero, J. *J. Mol. Struct.* **2008**, *891*, 325−328.
(45) Bauta, W. E.; Lovett, D. P.; Cantrell, W. R., Jr.; Burke, B. D. *J. Org. Chem.* **2003**, *68*, 5967−5973.
(46) Pelter, A.; Elgendy, S. *Tetrahedron Lett.* **1988**, *29*, 677−680.
(47) Rathke, M. W.; Cowan, P. J. *J. Org. Chem.* **1985**, *50*, 2622−2624.
(48) Kornblum, N.; Smiley, R. A.; Blackwood, R. K.; Iffland, D. C. *J. Am. Chem. Soc.* **1955**, *77*, 6269−6280.
(49) Nicolaou, K. C.; Estrada, A. A.; Zak, M.; Lee, S. H.; Safina, B. S. *Angew. Chem., Int. Ed.* **2005**, *44*, 1378−1382.
(50) (a) Tamura, Y.; Wada, A.; Kita, Y. *Tetrahedron Lett.* **1981**, *22*, 4283−4286. For a review on cyclic anhydrides in cycloaddition reactions, see: (b) González-López, M.; Shaw, J. T. *Chem. Rev.* **2009**, *109*, 164−189.
(51) (a) Ohta, Y.; Hirose, Y. *Chem. Lett.* **1972**, 263−266. For a discussion on the role of the counterion in cationic cyclizations, see: (b) Pronin, S. V.; Shenvi, R. A. *Nat. Chem.* **2012**, *4*, 915−920.
(52) Yamaguchi, S.; Nedachi, M.; Yokoyama, H.; Hirai, Y. *Tetrahedron Lett.* **1999**, *40*, 7363−7365.
(53) (a) Raczyńska, E. D.; Kosińska, W. *Chem. Rev.* **2005**, *105*, 3561−3612. (b) Cyrański, M. K. *Chem. Rev.* **2005**, *105*, 3773−3811. (c) Korth, H.-G.; Mulder, P. *J. Org. Chem.* **2013**, *78*, 7674−7682.
(54) Barton, D. H. R.; Ley, S. V.; Magnus, P. D.; Rosenfeld, M. N. *J. Chem. Soc., Perkin Trans. 1* **1977**, 567−572.
(55) Crystallographic data for compounds **60** (CCDC 941202), 15-*epi*-**133** (CCDC 941203), and **1** (945867) have previously been reported by us (see ref 28). These data can be obtained free of charge from The Cambridge Crystallographic Data Centre via www.ccdc.cam.ac.uk/data_request/cif.
(56) For the sake of clarity, and because fragment **111** is racemic, we elected to define the newly generated stereocenters at C4 and C4a as those shown in Scheme 20, which results in the configuration at C15 appearing as a mixture (hence 15-*epi*). Both diastereomers shown are formed along with their enantiomeric counterparts.
(57) Kahne, D. E. Ph.D. Thesis, Columbia University, 1986.
(58) (a) White, J. D.; Nolen, E. G., Jr.; Miller, C. H. *J. Org. Chem.* **1986**, *51*, 1150−1152. (b) White, J. D.; Demnitz, F. W. J.; Xu, Q.; Martin, W. H. C. *Org. Lett.* **2008**, *10*, 2833−2836.
(59) Fitzjarrald, V. P.; Pongdee, R. *Tetrahedron Lett.* **2007**, *48*, 3553−3557.
(60) Alternative batches of material displayed varying diastereomeric ratios ranging from 1:1 to 3:1, favoring the desired C15 spirocycle configuration, albeit in reduced yield, indicating some levels of diastereomeric enhancement during chromatography.
(61) Gioeli, C.; Balgobin, N.; Josephson, S.; Chattopadhyaya, J. B. *Tetrahedron Lett.* **1981**, *22*, 969−972.
(62) (a) Corey, E. J.; Yang, Y. K. *Tetrahedron Lett.* **1992**, *33*, 2289−2290. (b) Nicolaou, K. C.; Reddy, K. R.; Skokotas, G.; Sato, F.; Xiao, X. Y.; Hwang, C. K. *J. Am. Chem. Soc.* **1993**, *115*, 3558−3575.
(63) Denmark, S. E.; Kobayashi, T.; Regens, C. S. *Tetrahedron* **2010**, *66*, 4745−4759.
(64) Fürstner, A.; Weintritt, H. *J. Am. Chem. Soc.* **1998**, *120*, 2817−2825.
(65) Adam, W.; Smerz, A. K. *Tetrahedron* **1996**, *52*, 5799−5804.
(66) Davis, F. A.; Stringer, O. D. *J. Org. Chem.* **1982**, *47*, 1774−1775.
(67) (a) Ikota, N.; Ganem, B. *J. Org. Chem.* **1978**, *43*, 1607−1608. (b) Clarembeau, M.; Cravador, A.; Dumont, W.; Hevesi, L.; Krief, A.; Lucchetti, J.; Van Ende, D. *Tetrahedron* **1985**, *41*, 4793−4812. (c) Krief, A.; Hobe, M.; Badaoui, E.; Bousbaa, J.; Dumont, W.; Nazih, A. *Synlett* **1993**, 707−709. (d) Santi, C.; Santoro, S.; Testaferri, L.; Tiecco, M. *Synlett* **2008**, 1471−1474.
(68) (a) Donohoe, T. J.; Blades, K.; Moore, P. R.; Waring, M. J.; Winter, J. J. G.; Helliwell, M.; Newcombe, N. J.; Stemp, G. *J. Org. Chem.* **2002**, *67*, 7946−7956. (b) Donohoe, T. J.; Bataille, C. J. R. *Org. React.* **2012**, 1−48.
(69) Phillips, S. T.; Shair, M. D. *J. Am. Chem. Soc.* **2007**, *129*, 6589−6598.
(70) Schadt, F. L.; Bentley, T. W.; Schleyer, P. v. R. *J. Am. Chem. Soc.* **1976**, *98*, 7667−7674.
(71) Experimental evidence has been reported that supports the existence of a transient, ring-opened intermediate. See: (a) Hlavka, J. J.; Bitha, P.; Boothe, J. H. *J. Am. Chem. Soc.* **1968**, *90*, 1034−1037. (b) Scott, A. I.; Yamaguchi, E.; Chung, S.-K. *Tetrahedron Lett.* **1975**, *16*, 1369−1372. For related rearrangements, see: (c) Stork, G. *Chem. Ind.* **1955**, 915−916. (d) Barton, D. H. R.; Scott, A. I. *J. Chem. Soc.* **1958**, 1767−1772.
(72) Miller, B. *Acc. Chem. Res.* **1975**, *8*, 254−256.
(73) Horiuchi, C. A.; Ji, S. J.; Matsushita, M.; Chai, W. *Synthesis* **2004**, 202−204.
(74) Mukaiyama, T.; Matsuo, J.; Kitagawa, H. *Chem. Lett.* **2000**, *29*, 1250−1251.
(75) Tatsuta, K.; Fukuda, T.; Ishimori, T.; Yachi, R.; Yoshida, S.; Hashimoto, H.; Hosokawa, S. *Tetrahedron Lett.* **2012**, *53*, 422−425.
(76) (a) Köster, R.; Seidel, G. In *Organometallic Syntheses*; King, R. B.; Eisch, J. J., Eds.; Elsevier: Amsterdam, 1998; Vol. *4*, pp 440−442. (b) Fürstner, A.; Seidel, G. *J. Org. Chem.* **1997**, *62*, 2332−2336.
(77) Gibert, M.; Ferrer, M.; Sánchez-Baeza, F.; Messeguer, A. *Tetrahedron* **1997**, *53*, 8643−8650.
(78) Professor Yi Tang (UCLA) is acknowledged for providing natural viridicatumtoxin A [(+)-**2**] obtained from *P. aethiopicum*. In this study, that material was used for antibacterial testing. For the comparison data, compound (+)-**2** was isolated by Kim and co-workers from *Penicillium* sp. FR11 (see ref 1).
(79) Nelson, M.; Hillen, W.; Greenwald, R. A. *Tetracyclines in Biology, Chemistry, and Medicine*; Birkhauser Verlag: Basel, 2001; p 26.
(80) (a) Oliva, B.; Gordon, G.; McNicholas, P.; Ellestad, G.; Chopra, I. *Antimicrob. Agents Chemother.* **1992**, *36*, 913−919. (b) Chopra, I. *Antimicrob. Agents Chemother.* **1994**, *38*, 637−640.
(81) The Clinical and Laboratory Standards Institute (CLSI) defines a bactericidal compound as one capable of inducing a ≥ 3 $\log_{10}$ drop in colony-forming units (CFU)/mL.
(82) Jenner, L.; Starosta, A. L.; Terry, D. S.; Mikolajka, A.; Filonava, L.; Yusupov, M.; Blanchard, S. C.; Wilson, D. N.; Yusupova, G. *Proc. Natl. Acad. Sci., U. S. A.* **2013**, *110*, 3812−3816.

(83) For a recent review on the role of chemical synthesis in antibacterial drug discovery, see: Wright, P. M.; Seiple, I. B.; Myers, A. G. *Angew. Chem., Int. Ed.* **2014**, DOI: 10.1002/anie.201310843.